TALLINN UNIVERSITY OF TECHNOLOGY
SCHOOL OF ENGINEERING
Department of Civil Engineering and Architecture

DEGRADATION OF TOLUENE IN GASEOUS PHASE BY PULSED CORONA DISCHARGE FOLLOWED BY PHOTOCATALYTIC OXIDATION

TOLUEENI LAGUNDAMINE GAASIFAASIS KOROONA-IMPULSS ELEKTRILAHENDUSEGA KOOS JÄRGNEVA FOTOKATALÜÜTILISE OKSÜDATSIOONIGA

MASTER THESIS

Student:	Daniel Anselm Teittinen
Student code:	223604EABM
Supervisor:	Juri Bolobajev, Senior lecturer

Tallinn 2024

AUTHOR’S DECLARATION

Hereby I declare, that I have written this thesis independently.
No academic degree has been applied for based on this material. All works, major viewpoints and data of the other authors used in this thesis have been referenced.

“.......” .... 20…..

Author: Daniel Anselm Teittinen
/signature /

Thesis is in accordance with terms and requirements

“.......” January 2024

Supervisor: …..........................
/signature/

Accepted for defence

“.......”....................20… .

Chairman of theses defence commission: ....
/name and signature/

Non-exclusive licence for reproduction and publication of a graduation thesis[1]

I, Daniel Anselm Teittinen (16.03.1999)

1. grant Tallinn University of Technology free licence (non-exclusive licence) for my thesis Degradation of toluene in gaseous phase by pulsed corona discharge followed by photocatalytic oxidation,
(*title of the graduation thesis*)

supervised by Juri Bolobajev
(*supervisor's name*)

1.1 to be reproduced for the purposes of preservation and electronic publication of the graduation thesis, incl. to be entered in the digital collection of the library of Tallinn University of Technology until expiry of the term of copyright;

1.2 to be published via the web of Tallinn University of Technology, incl. to be entered in the digital collection of the library of Tallinn University of Technology until expiry of the term of copyright.

2. I am aware that the author also retains the rights specified in clause 1 of the non-exclusive licence.

3. I confirm that granting the non-exclusive licence does not infringe other persons' intellectual property rights, the rights arising from the Personal Data Protection Act or rights arising from other legislation.

______________ (date)

---

[1] *The non-exclusive licence is not valid during the validity of access restriction indicated in the student's application for restriction on access to the graduation thesis that has been signed by the school's dean, except in case of the university's right to reproduce the thesis for preservation purposes only. If a graduation thesis is based on the joint creative activity of two or more persons and the co-author(s) has/have not granted, by the set deadline, the student defending his/her graduation thesis consent to reproduce and publish the graduation thesis in compliance with clauses 1.1 and 1.2 of the non-exclusive licence, the non-exclusive license shall not be valid for the period.*

Department of Civil Engineering and Architecture

THESIS TASK

Student: Daniel Anselm Teittinen, 203604EABM
Study programme,
main speciality: EABM03/22 - Environmental Engineering and Management
Supervisor: Senior lecturer, Juri Bolobajev, 6202855

Thesis topic:
(in English) Degradation of toluene in gaseous phase by pulsed corona discharge followed by photocatalytic oxidation
(in Estonian) Tolueeni lagundamine gaasifaasis koroona-impulss elektrilahendusega koos järgneva fotokatalüütilise oksüdatsiooniga

Thesis main objectives:

1. Preparation of literature review according to master's plan
2. Development of test methodology and testing
3. Analysis and interpretation

Thesis tasks and time schedule:

No	Task description	Deadline
1.	Literature review	29.10.2023
2.	Materials and methods	26.11.2023
3.	Results and discussion	31.12.2023

Language: English **Deadline for submission of thesis:** "05" January 2024

Student: Daniel Anselm Teittinen .... "......." January 2024
/signature/
Supervisor: Juri Bolobajev .... "......." January 2024
/signature/
Head of study programme: Karin Pachel .... "......." January 2024
/signature/

Terms of thesis closed defence and/or restricted access conditions to be formulated on the reverse side

CONTENTS

PREFACE

The subject of this thesis is oxidation of toluene in air mixtures by pulsed corona discharge followed by photocatalytic oxidation. This topic was proposed by my supervisor Juri Bolobajev (Senior lecturer), who consulted me, helped with the selection of sources and calculations. He also checked the work, and I am thankful for the help and inspiration of my supervisor. It has been a pleasure to work with such a professional supervisor. Experimental work was conducted at Tallinn University of Technology Laboratory of Environmental Technology.

I would like to express additional thanks to Viktoria Voronova (Senior lecturer) who made it possible to have an interesting internship and international projects during my master’s studies. All my fellow students Kimmo, Micah, Ann, Markos, Marlen, Triin and Anette in the master’s program deserve an applause for their support, joy, and enthusiasm.

Keywords: Air purification, toluene degradation, pulsed corona discharge, photocatalytic oxidation, master thesis.

Tallinn,
January 2024
Daniel Teittinen

List of abbreviations

AOP	Advanced oxidation processes
BTEX	Benzene, toluene, ethylbenzene and xylene
EEA	European Environment Agency
EPA	U.S. Environmental Protection Agency
EPER	European Pollutant Emission Register
Eq.	Equation
EU	The European Union
FTIR	Fourier transform infrared spectroscopy
HPLC	High-performance liquid chromatography
ICE	Internal combustion engines
LEL	Lower explosive limit
LOAEL	Lowest Observed Adverse Effect Level
MRL	Minimal risk level
NEC	National emissions reduction commitments
NMVOC	Non-methane volatile organic compounds
NTP	Non-thermal plasma
PCD	Pulsed corona discharge
PCO	Photocatalytic oxidation
PEL	Permissible exposure limits
ppb	One part per billion
ppm	One part per million
pps	Pulses per second
SRT	Specific residence time
TVL	Threshold limit value
TWA	Time-weighted average
UV	Ultraviolet
VOC	Volatile organic compounds
WHO	World Health Organization

1. INTRODUCTION

Volatile organic compounds (VOCs) emission is considered as one of the five main air pollution problems in the European Union (EU) along with nitrogen oxides (NOx), sulphur dioxide (SO_2), ammonia (NH_3), and fine particulate matter ($PM_{2.5}$) emissions (2016/2284/EU). Main pollution sources of VOCs in Estonia include industries, agriculture, and residential areas (EEA 2023). VOC concentrations are often high in buildings, which could pose adverse health effects on residents and workers (Bolden et al. 2015, Geiss et al. 2011). Among the most widely used VOCs are aromatic hydrocarbons like benzene, toluene, ethylbenzene, and xylene (BTEX). Prolonged exposure to VOCs may cause asthma and other respiratory diseases even at low concentrations (Sharma 2018).

Technologies for VOC removal from air include incineration, absorption and adsorption, condensation, and biological treatment processes. High energy consumption and poor adaptability for various VOC concentrations present challenges for conventional treatment methods. Pulsed corona discharge (PCD) combined with photocatalytic oxidation (PCO) provides an energy efficient solution for the abatement of VOCs at low concentrations (Feng et al. 2017).

Further development and deeper understanding of the PCD process combined with PCO is needed. In this thesis toluene degradation with PCD followed by PCO treatment was studied. The literature review allowed to examine toluene as an air pollutant and review current VOC removal technologies considering their advantages and disadvantages. Experiments with artificially polluted air was carried out in controlled laboratory conditions. The objective of the experimental part was to investigate the toluene degradation in gas and water phases implementing PCD and PCO treatment. Additionally, the efficiency of toluene removal in the PCD and PCO processes was evaluated based on experimental results. Finally, ozone conversion kinetics in PCO was discussed.

Better understanding of the oxidation processes enables more efficient reactor designs and gives more credibility for the PCD process combined with PCO. Successful implementation of the technology will ensure cleaner urban and indoor air leading to healthier living and working environments for all.

2. LITERATURE REVIEW

Urbanization and industrialization have increased emissions of volatile organic compounds. VOC emissions in the atmosphere contribute to the formation of secondary pollutants, which lead to decreased air quality and contribute to the forming of photochemical smog that has severe health effects on both humans and damages the nature.

Generally, VOCs refer to organic compounds with boiling points below 250 °C, which makes them easily volatile. VOCs include alkanes, alkenes, alkynes, aromatics, alcohols, aldehydes, ketones, esters, halocarbons, and sulphur or nitrogen containing compounds. In the atmosphere VOCs form secondary pollutants, such as tropospheric ozone, peroxyacetyl nitrate and secondary organic aerosols. These compounds are toxic and carcinogenic to humans. Especially aromatics, such as benzene and toluene, and alkenes are recognized as highly polluting molecules because of their contribution in photochemical ozone formation. Additionally, halogenated and chlorinated VOCs are chemically stable and inherently toxic. (He *et al.*, 2019.)

In the following sections, toluene and more generally VOCs are examined with regards to their sources, their typical concentrations in urban air and indoors, health impacts, guidelines, and regulations. Currently used technologies for VOC removal, including incineration, adsorption, absorption, condensation, and biological treatment are described and evaluated. At the end of the literature review, pulsed corona discharge and photocatalytic oxidation processes are described.

2.1 Toluene as BTEX chemical

Toluene (methylbenzene) is a colourless aromatic compound with molecular weight of 92.14 g·mol^{-1}. In atmospheric pressure, the melting and boiling points of toluene are -94.9 °C and 110.6 °C, respectively. Even in room temperature toluene is highly volatile and has a specific odour. Toluene is flammable and toxic and it should be handled carefully.

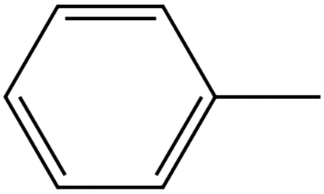

Figure 1. Chemical structure of toluene C_7H_8.

Toluene contains aromatic ring and a methyl group CH_3. Aromatic ring is a stable molecular structure, which makes BTEX group compounds difficult to be removed from waste streams. Either a high temperature or a strong oxidant is needed to destroy the molecular structure of aromatic ring.

2.1.1 Sources of toluene

Toluene rarely occurs individually as a pollutant, rather it is emitted with other aromatic hydrocarbons and VOCs. There is a wide variety of industries that release VOC emissions. The character of an industry determines the types of VOCs that are emitted. Identified sources of VOCs include petroleum refining, polymer, solvent and fine chemical industries, synthetic resin production, textile dyeing and printing, printing ink production, leather manufacturing, pharmaceutical industry, pesticide manufacturing, coating and adhesive manufacturing, spraying, and the manufacture of electronic equipment (He *et al.*, 2019). The list of industries show that manufacturing and extractive industries are the largest sources of emissions. Agricultural VOC emissions are associated with pesticide use. With regards to residential, commercial and institutional VOC emissions, many of the industrial activities can also be associated with this sector, namely printing and dyeing, solvent, and fine chemical use. These activities could take place in offices, homes and garages or workshops.

Aromatic hydrocarbons are one of the most typical VOCs, attributed to most of the abovementioned emissions sources. Among aromatic hydrocarbons, benzene, toluene, ethylbenzene and xylenes (BTEX) contribute to the majority of the total industrial emissions. Wang *et al.* (2007) recognized several indoor sources of aromatic hydrocarbons such as paints, adhesives, gasoline, combustion sources, and even smoking. Cheng and Brown (2003) identified that the largest sources of indoor VOCs are building materials, surface finishes, and appliances, such as gas heaters and electric ovens.

Emissions of NMVOCs (non-methane volatile organic compounds) are reported in European Union (EU) according to National Emissions reduction Commitments (NEC) Directive (2016/2284/EU). In Estonia in 2021, the total NMVOC emissions equalled to 26.51 Gg or 26 510 Mt (figure 1). For 2030, Estonia has the target to reduce NMVOC emissions to 20 Gg. The figure 1 shows that more than half of the emissions, almost 15 Gg, come from manufacturing and extractive industry (56.4 %). Other important emission sources are agriculture (17.7 %) as well as residential, commercial, and institutional (12.0 %) sectors. To a lesser extent energy supply (7.2 %) and transport (5.8 %) also cause emissions. A marginal amount of NMVOCs is emitted from the waste sector (0.8 %).

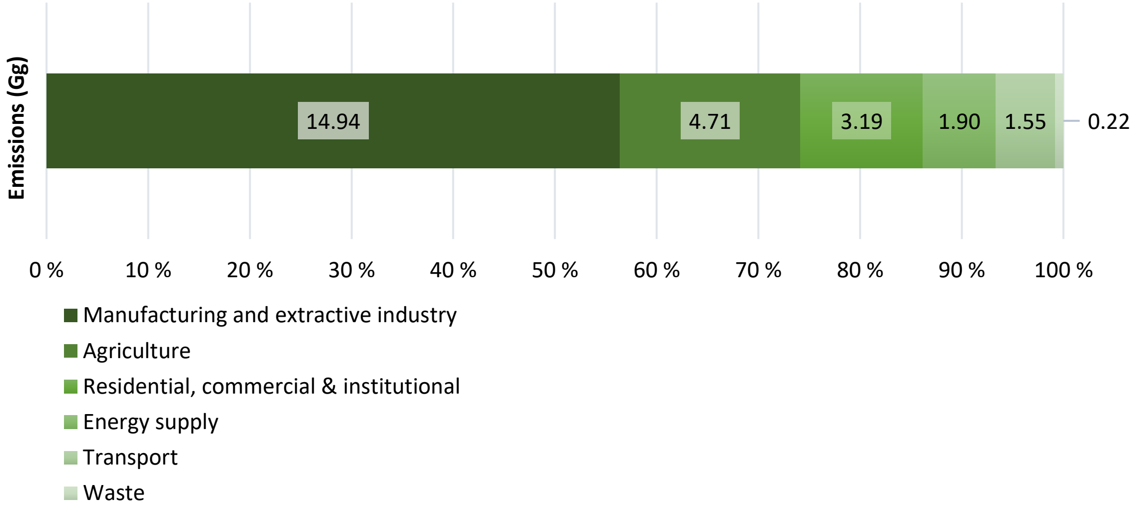

Figure 1. NMVOC emissions in Estonia in 2021 from various sectors (EEA 2023).

VOCs and BTEX are well known pollutants which is why there are many studies and campaigns measuring their concentration both outdoors and inside buildings. Some of the studies reporting the concentrations of toluene are discussed next.

2.1.2 Reported concentrations of toluene indoors and in the atmosphere

A European study called AIRMEX (Geiss et al. 2011) carried out measuring campaigns in public buildings in urban areas with high traffic density and in kindergartens and schools situated in suburbs with medium traffic impact. Approximately 1000 samples were taken from 182 different working environments and private homeplaces including in total 10 European cities. Concentrations for toluene are presented in table 1.

Table 1. Concentrations of toluene in public and private spaces in European cities (Geiss et al 2011).

Space	Values (n)	Min ($\mu g \cdot m^{-3}$)	Max ($\mu g \cdot m^{-3}$)	Median ($\mu g \cdot m^{-3}$)	P95 ($\mu g \cdot m^{-3}$)
Outdoor (ambient)	108	0.8	207.8	4.8	33.2
Public buildings/schools	188	1	103.8	7.1	47.6
Private houses	96	1.3	160.6	6.5	28.4
Personal exposure	146	1.4	291	11.7	55.3

Table 1 shows that the lowest toluene concentration was measured in private houses as well as outdoors. This is expected because the pollutants quickly disperse in the atmosphere. The median toluene concentration of 108 outdoor samples is 4.8 $\mu g \cdot m^{-3}$ (2.4 ppb). In personal exposure the median concentration is 11.7 $\mu g \cdot m^{-3}$ (5.9 ppb). Personal exposure concentrations are more than double compared to the outdoor concentrations. The 95th percentile concentration of the personal exposure was the highest with 55.3 $\mu g \cdot m^{-3}$ (27.9 ppb). Public buildings, private houses, and personal working spaces have generally higher concentrations of toluene compared to ambient concentrations. Therefore, considering toxic and carcinogenic properties of toluene and a high probability of its presence indoors special attention should be placed on the development of state-of-the-art air cleaning systems, which are targeted to get rid of this pollutant from indoor air. Outdoors the main source of pollutants is traffic, more specifically the incomplete combustion in internal combustion engines (ICE). Replacing ICEs by electrical engines, will likely improve urban air quality in the coming decades.

Wallenius et al. (2022) reported toluene concentrations in Finnish office and non-industrial indoor environments in 2010-2019. The findings show that among the hydrocarbons, toluene is frequently found in air samples (81 % of the samples). In total 9789 air samples were taken from offices, schools, kindergartens and healthcare offices during a ten-year research program. In the samples the median concentration of toluene was 0.7 $\mu g \cdot m^{-3}$, 95th percentile was 5.0 $\mu g \cdot m^{-3}$, and the maximum concentration observed was 620 µg·m^{-3}. Compared to the AIRMEX study results for public buildings and schools in table 1, the concentrations reported by Wallenius *et al.* (2022) were smaller by one factor. This indicates that the air quality between the major European and Finnish cities differs.

These two studies show that there are regional differences of VOC concentrations, which largely depend on the local industry, amount of traffic, and other relevant sources such as used building materials. While much can be done to decrease the overall VOC emissions, efficient means are also needed to remediate the VOC pollution in indoor air. If appropriate actions are not taken, the toluene and VOCs can risk human health. The effects of toluene on human health will be described in the next section.

2.1.3 Common exposure to toluene and its negative impact on human health

Aromatic hydrocarbons are hazardous substances possessing toxic and carcinogenic properties to humans. Especially benzene has been recognized as a hazardous compound even in small concentrations. Toluene is another commonly used solvent in the chemical industry and a significant contributor to the formation of photochemical smog. Even a few parts per million (ppm) concentration of VOCs in air can cause long-term diseases such as asthma and reduced lung capacity if a person is exposed to polluted air for long time periods. Generally, VOCs are considered carcinogenic compounds to humans (Sharma *et al.* 2018). However, the International Agency for Research on Cancer determined that toluene is not classifiable as to its carcinogenicity in humans and The United States Environmental Protection Agency (EPA) determined that there is inadequate information to assess the carcinogenic potential of toluene. Thus, toluene is not considered a carcinogenic substance (ATSDR 2017).

VOCs in the atmosphere contribute to elevated tropospheric (ground-level) ozone concentrations. As a secondary pollutant tropospheric ozone has several harmful effects on human health. United States (U.S.) Environmental Protection Agency (EPA 2023) listed health problems caused by ozone including coughing, sore throat, difficulty to breathe deeply, pain when breathing, inflammation, and damage of airways. Ozone is also aggravating lung diseases such as asthma, emphysema and chronic bronchitis, as well as increasing the frequency of asthma attacks. At the highest risk of these health effects are children whose lungs are not fully developed, outdoor workers, and older adults.

Exposure to toluene has been correlated with endocrine disruption, skin symptoms, respiratory sicknesses, alterations in immune system, and cardiovascular disease (Bolden, Kwiatkowski and Colborn 2015). Serious health effects of toluene are often associated with solvent abuse meaning individuals who smoke or intentionally inhale products containing toluene for its euphoric effects. Temporary effects of toluene on nervous system include headaches, dizziness or unconsciousness. With repeated exposure permanent effects such as cognitive impairment, incoordination, vision and hearing loss may occur. Day-to-day exposure to moderate levels of toluene at workplace can cause tiredness, confusion, weakness, drunken-type actions, memory loss, nausea, and loss of appetite. Hearing and colour vision loss can be long-term effects of moderate exposure to toluene. (ATSDR 2017.)

2.1.4 Public health guidelines and government regulations towards toluene

In the European Union (EU) VOC emissions are regulated by Air Quality Directive (2008/50/EC) and National Emissions reduction Commitments (NEC) directive (2016/2284/EU). Directive sets reduction commitments for five main air pollutants: NO_x, NMVOCs, SO_2, NH_3 and $PM_{2.5}$. NMVOC reduction commitments are also relevant for toluene emissions. European Environment Agency (EEA) monitors and publishes data about the status of emissions in the EU. Larger than 200 kg per year of BTEX emissions must be reported to the European Pollutant Emission Register (EPER). Ambient Air Quality Directive (2008/50/EC) sets annual average limit value for benzene emissions as 5 $\mu g \cdot m^{-3}$ but toluene is only mentioned in connection with measurements of ozone precursor substances. In the directive, there are no emission limits specifically for toluene.

The U.S. Agency for Toxic Substances and Disease Registry (ATSDR) has derived minimal risk levels (MRLs) for toluene in a comprehensive report "Toxicological profile for Toluene" (ATSDR 2017). MRLs are substance-specific estimates that are intended to serve as screening levels and are used by health assessors to identify potential health effects of contaminants. Acute-duration inhalation MRL for toluene is 2 ppm (7.6 $mg \cdot m^{-3}$) for exposure durations up to 14 days. Acute-duration exposure is based on the lowest-observed-adverse-effect level (LOAEL) for minimally adverse neurological effects in humans. For time periods greater than 365 days the chronic-duration inhalation MRL is 1 ppm (3.8 $mg \cdot m^{-3}$) based on the no-observed-adverse-effect level (NOAEL) for neurological effects in humans.

The American Conference of Governmental Industrial Hygienists (ACGIH) recommends an 8-hour time-weighted average (TWA) threshold limit value (TLV) of 20 ppm toluene to protect against visual impairment and female reproductive effects including pregnancy loss. National Institute for Occupational Safety & Health (NIOSH) in the U.S. recommends that 100 ppm exposure limit should not be exceeded at any time and determined that 500 ppm limit value is immediately dangerous to life and health. (ATSDR 2017.)

ATSDR, ACGIH, and NIOSH give recommendations, which are not enforced by laws. Occupational Safety and Health Administration (OSHA) determines regulatory limits for hazardous substances in the U.S. called permissible exposure limits (PELs). Work practices and engineering controls need to be instituted to stay at or below the PELs. According to PEL for toluene the employer must ensure that employee’s exposure does not exceed TWA of 200 ppm in an 8-hour work shift. The ceiling concentration that shall not be exceeded at any time during an 8-hour shift is 300 ppm and the acceptable maximum peak is 500 ppm for 10 minutes. (ATSDR 2017.)

World Health Organization (WHO) has not established any air quality guidelines for toluene but sets a health-based drinking water guideline for toluene at 0.7 $mg \cdot L^{-1}$. The U.S Food and Drug Administration (FDA) has set a limit for toluene in drinking water as 1 $mg \cdot L^{-1}$.

2.2 Available technologies for the recovery and removal of VOCs

Due to the adverse effects of BTEX chemicals and VOCs in general, reducing VOC emissions has become an important target for all associated industries. The legislation in the EU also sets requirements and targets for recommended emission levels. Reducing emissions can be achieved by recovery technologies within the process boundaries or by destroying the pollutants before releasing the waste flows into the environment. Recovery technologies include adsorption and absorption, membrane separation and condensation. Recovery of chemicals reduces the amount of VOC emissions due to higher efficiency in raw-material use. It is possible to recover some of the chemicals in the production using these methods, but there are issues related to disposal of spent solvents and materials used in the process, or high energy consumption in the case of membrane separation. (He *et al.* 2019.) Membrane processes and condensation are more suitable for gas cleaning with high concentration of pollutants. For indoor air purification, where concentration does not usually exceed 10 ppm, methods with higher efficiency are required.

Compounds that are not recovered from the processes become pollutants in the waste streams of industries. There are several end-of-pipe technologies utilized for VOCs removal. Pollutants can be destroyed from the waste flows by thermal oxidation. A catalyst can be used to lower the temperature needed for the incineration, which increases the energy efficiency of the process. Biological degradation of the pollutants is possible in some cases. Advanced oxidation methods include photocatalytic oxidation and non-thermal plasma, which are discussed in more detail in section 2.3.

2.2.1 Incineration and thermal catalytic oxidation

Incineration of VOCs is simple and efficient, but requires very high temperatures to achieve full oxidation, above 800 °C. Maintaining high temperatures during incineration makes this technology energy consuming and thus unfeasible in terms of green technologies application. Auxiliary fuel is often needed to reach high temperatures. If fossil fuels such as natural gas is used, cleaning the polluted stream produces additional carbon dioxide emissions.

Toluene has auto-ignition temperature of 552 °C in which toluene will ignite without any external source. It is suggested that the design temperature of incinerator would be few hundred degrees above the VOCs auto-ignition temperature (Chiang and Gao 2022).

Adding a suitable catalyst to the exhaust enables the oxidation at temperature around 200 °C – 500 °C, depending on the waste stream characteristics, catalytic material type, and reactor design used in the process. Catalytic degradation of VOCs is effective for the removal of dilute (<0.5 vol. %) VOC effluents. (He *et al.*, 2019.)

In thermal catalytic oxidation there are many parameters affecting the suitability and feasibility of catalysts for a certain application. A good catalyst should have a high activity and stability in addition of being durable and possible to regenerate. Catalysts can be poisoned by the reaction products as well as other undesirable substances in the waste stream. Coking and thermal sintering are other common problems with catalysts. Several approaches are available for catalyst regeneration such as heat treatment, ozone oxidation, chemical regeneration, and oxygen plasma treatment. Regeneration of a catalyst can recover the catalytic activity but sometimes catalysts are irreversibly damaged, as in the case of chemical sintering. Replacing catalysts create additional costs and waste. (He et al. 2019.)

The feasibility of thermal combustion can be determined by calculating the lower explosive limit (LEL) concentration of the gas mixture. For thermal catalytic oxidation and incineration LEL should be between 15–20 % and 20–25 %, respectively (Chiang and Gao 2022). If the gas composition is known, LEL can be calculated with the following equation 1.

$$c_m = \frac{100}{\frac{x_1}{c_1} + \frac{x_2}{c_2} + \cdots + \frac{x_3}{c_3}} \tag{1}$$

where c_m – lower explosive limit of mixture,
c_i – lower explosive limit of a component, and
x_i – mass percentage of the component in the mixture.

Combustion kinetics can be expressed by the equations 2.1, 2.2, and 3 (Noll 1999).

$$-\left(\frac{dC_A}{dt}\right) = k \cdot C_A \tag{2.1}$$

$$ln\left(\frac{C_A}{C_{A0}}\right) = -kt \tag{2.2}$$

$$k = A \cdot e^{-\frac{E}{RT}} \tag{3}$$

where C_A – concentration of compound A at the moment t,

C_{A0} – initial concentration of A at t=0,

A – frequency factor, s^{-1},

E – activation energy, kJ·g-mole^{-1},

R – gas constant, R = 8.314 J·(mol·K)$^{-1}$, 1.987 cal·(mol·K)$^{-1}$,

T is absolute temperature, K.

Thermal oxidation parameters based on first- order reaction kinetics are available in the literature for different compounds. For toluene $A = 2.28 \cdot 10^{13}$, E = 56.5 kcal/mol (Noll 1999). Based on equations 2.2 and 3 it is possible to calculate the required time for toluene combustion in a certain temperature. At a temperature of 677 °C (950 K) approximately 2 seconds are needed for 99 % toluene removal. Subsequent calculations can be made to estimate the required energy and auxiliary fuel demand to maintain high temperatures.

Incineration is a suitable pollutant removal method only for high concentration VOC streams that cannot be feasibly recovered due to its energy intensity. On the other hand, adsorption and absorption are processes that usually take place in ambient temperatures, which reduces the energy intensity of VOC removal. These processes are described in the next section.

2.2.2 Adsorption and absorption

Adsorption is an end-of-pipe technology that can effectively remove pollutants from the gaseous and liquid waste flows. Adsorption is used for the removal of sulphur and nitrogen oxides and VOCs from gaseous streams. Adsorbent is used to attract and bind pollutants to a solid adsorbent material such as activated carbon or zeolite. Attractive forces of an adsorbent are weaker than the chemical bonds of molecules. Thus, the pollutants are not destroyed during adsorption but simply captivated to the adsorbent surface. Adsorbent needs to be changed or regenerated as it is saturated with pollutants. Adsorption capacity depends on the adsorbent material as well as the characteristics of the polluted fluid flow. Concentration of pollutants, molecular weight, diffusion coefficient, polarity and boiling point are parameters that affect the adsorption of gases. (Chiang and Gao 2022.)

During the adsorption the gas flow is directed through a bed of solid materials with good adsorption properties. Activated carbon, synthetic ion exchange resins, and some inorganic oxides can be used as adsorbents. Granular Activated Carbon (GAC) and zeolite are examples of commercial adsorbents for VOCs removal. Bed material gets saturated with pollutants over time. When the adsorbent is fresh, it has the highest adsorption capacity and captivates almost all the pollutants from the waste flow. When the adsorbent gets saturated there is no difference in pollutant concentration between adsorption inlet and outlet. This is described as the breakthrough of the gas flow. Breakthrough curve can be drawn to illustrate the capacity of adsorbent material during the process. (Chiang and Gao 2022.)

Figure 2 shows how the pollutant concentration at the outlet remains zero for 20 minutes, after which the concentration starts to rise until it reaches close to 100 per cent concentration in about 40 minutes. Usually, the pollutant concentration is not allowed to climb over some limit value, which can also be described as the breakthrough point of the pollutant. Staying below the limit values require frequent replacing or regenerating of the bed material which can be material and energy intensive as well as expensive. With low pollutant concentration or a larger adsorption column the lifetime of bed material will be longer.

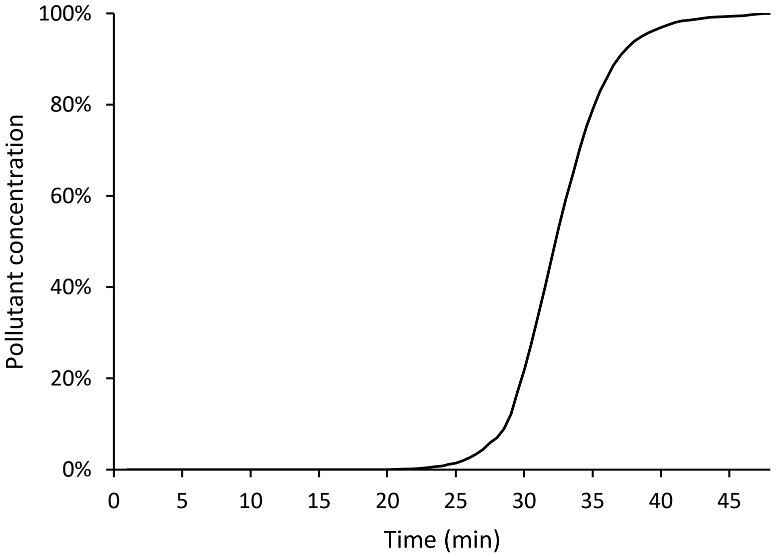

Figure 2. Breakthrough curve of an adsorption column (Frascari et al. 2019, modified by Daniel Teittinen).

Instead of capturing the pollutants on solids as in adsorption, absorption is the selective transfer of molecules from gas to liquid solvent. VOCs that have high solubility for the solvent that is used as absorbent can be extracted from the gas flow. The outlet concentration of the pollutant should be 500 to 5 000 ppm or higher to create a sufficient concentration difference between gas and liquid phase. Contact area between gas and liquid phases need to be maximised for efficient mass transfer. Henry's law describes the equilibrium between gaseous and liquid phases in adsorption process (Eq. 4). (Chiang and Gao 2022.)

$$C = k_H P \tag{4}$$

where C – solubility of a gas in the solvent, M,
k_H – Henry's law constant, M·atm^{-1},
P – partial pressure of the gas, atm.

By increasing the gas side pressure or lowering the liquid temperature, it is possible to increase the solubility of a gas in the solvent. Water is most commonly used as a solvent, but some VOCs such as toluene and benzene have very low solubility in water. Solubilities in water are 0.47 to 0.56 g·L^{-1} and 1.75 to 1.80 g·L^{-1} for toluene and benzene, respectively (SciFinder 2023). Low solubility makes the use of absorption unsuitable for their recovery.

2.2.3 Condensation

Condensation enables the recovery of gaseous waste streams by lowering the temperature of the compounds below the boiling point. Condensation is efficient for VOCs with boiling points above 40 °C and concentrations above 5 000 ppm (Chiang and Gao 2022). Toluene has a high boiling point of 111 °C, but some hydrocarbons such as methane and ethane have low boiling points of −161 °C and −89 °C requiring very low temperature for condensation.

Low temperature condensation process is called cryogenic condensation. Liquid nitrogen has a boiling point of −195.8 °C, which makes it a suitable agent for cryogenic condensation of VOCs. In addition to the suitable boiling point, use of liquid nitrogen is inherently safe condensation technology due to the inert nature of nitrogen. Additional dehydration step is needed to remove water vapour before VOCs condensation. (Xu et al. 2023.)

Xu et al. (2023) proposed a VOCs recovery system which had low-temperature adsorption added to cryogenic condensation with liquid nitrogen. Most of the VOCs condensate to liquid in low temperature and are recovered. The remaining gaseous VOCs are directed through an activated carbon adsorption column where they are captured. This combination of technologies reached close to zero VOCs emissions. Cryogenic solutions are energy intensive due to extremely low temperatures used. Thus, the value of chemicals that can be recovered from the condensate needs to offset additional energy costs of the process.

2.2.4 Biological treatment

Microbial or biological treatment have important advantages compared to other VOCs removal methods. To support the growth of microbes the biological treatment is operated in mild conditions, which also save energy. Ideally the pollutants are converted to water, carbon dioxide and biomass, which are harmless products. Biological treatment can be used from high VOC concentration to low concentration pollution at only few ppm (Chiang and Gao 2022).

Problems faced with the biological treatment are mostly related to the microbial biomass. Sustaining microbes requires good nutrient, moisture, and pH control. The medium material supporting the biomass can be deteriorated over time. Moreover, clogging of the medium due to particulate matter is possible. The main types of biological reactors are biofilters, biotrickling filters, bioscrubbers, and membrane bioreactors. Different reactors use microorganisms either in suspended (liquid) or immobilized (biofilm) form depending on the pollutant type and concentration. (Mudliar et al. 2010.)

In biofilter bioreactor a humified air stream with pollutants goes through a porous column covered all over by a thin microbe layer. Microbes consume the organic compounds going through the filter in gaseous and liquid phase as the moisture condenses. Typical bed material for biofilter column are peat, soil, compost and wood chips. Compost and peat offer high organic matter content and high specific surface area in addition to good water holding capacity and permeability. Compost has additionally high level of intrinsic nutrients that are necessary for microbial growth. Downside of peat and compost is compacting due to high water holding capacity, which leads to increase in pressure drop over the bed column. Wood chips and bark are more stable materials to support the biofilter bed, but are lacking with regards to nutrient content, pH-buffering capacity and specific surface area. (Mudliar et al. 2010.)

The main difference with biotrickling filter to biofilter is that the nutrients are continuously provided by irrigating nutritious solution over the biofilter bed. Thus, the microorganisms are not dependant on the bed material as a source of nutrients. Therefore, inert materials can be used as growing medium. The bed material should be porous to give high specific surface area for microbial growth. Synthetic materials such as polyurethane have the highest specific surface area. Disadvantages of biotrickling filter are the accumulation of biomass in excess and secondary waste stream generated by the surplus nutrient solution that goes through the filter bed. (Mudliar et al. 2010.)

Bioscrubber has separate units for absorption and digestion of organic pollutants. In the absorption unit the pollutants are absorbed to liquid phase which is then pumped into bioreactor with microbial sludge. The bioreactor works with similar principle as activated sludge process in wastewater treatment with relatively stable operational conditions. Obvious downside of this technology is the excessive generation of sludge and liquid waste, which require further treatment.

Membrane bioreactor has a hydrophobic membrane, which selectively allows pollutants to pass from gas phase to a biofilm. The design of membrane bioreactor is simple compared to the first three technologies, requiring only the suitable membrane material to provide an interface between the gaseous and liquid phases. Biofilm grows on the membrane and a liquid flow over the biofilm provides all the nutrients necessary for microbial growth. Gas flows on the other side of the membrane and allows certain pollutants to pass to the biofilm. Membrane technology is especially useful for removing hydrophobic VOCs, which are not soluble to water, because the membrane allows high mass transfer between the biofilm and pollutants. (Mudliar et al. 2010.)

Biological treatment is a possible alternative for the removal of low to medium concentration of VOCs in a gas flow. Managing the microbial growth requires good control of important parameters such as moisture, nutrient, and pH to ensure high removal efficiency. Biotrickling filters and bioscrubbers require additional wastewater treatment due to separate liquid phase. All in all, biological treatment of VOCs can be used treat wide variety of organic and inorganic pollutants in industries and municipalities.

2.3 Explanation of processes used in the study

Advanced oxidation processes (AOPs) have been studied to develop more effective removal methods of pollutants in water and air. AOPs are water treatment processes utilizing hydroxyl radical •OH, which is a strong oxidant. A combination of two AOPs, pulsed corona discharge and photocatalytic oxidation, provides a novel solution for VOCs removal. The VOC pollutants are first destroyed in a non-selective process inside PCD reactor, after which the residual pollutants as well as ozone generated in the reactor are degraded to harmless compounds by photocatalytic reactor. A detailed description of the processes and their advantages and disadvantages are discussed in the following sections.

2.3.1 Pulsed corona discharge

Pulsed corona discharge is used to create conditions for non-thermal plasma (NTP) generation in a reactor. It is one of the most promising technologies in the control of VOCs. The characteristics and advantages of non-thermal plasma method are moderate operation conditions in ambient temperature and pressure, low cost, compact design, short residence time, and wide applicability for both high and low concentration VOCs. (Feng et al. 2018.)

NTP is ionized gas produced by high voltage electrical discharges. The plasma consists of electrons, ions, radicals, excited and neutral species, which interact with each other creating a highly reactive environment. Active species decompose pollutants to secondary and tertiary reaction products, optimally until complete mineralization to CO_2 and water. (Feng et al. 2018.)

Among the limitations of NTP are inferior product selectivity and the formation of undesired byproducts, which include ozone, NO_x, other VOCs, and aerosols. These can increase the toxicity of the treated gas stream. Coupling NTP with a photocatalytic reactor downstream from the NTP process can increase the overall quality and improve the efficiency of the process. Such an integrated system gives superior performance in terms of oxidation efficiency, reaction rate, and selectivity, when it is compared to a single NTP or a separate catalysic system. (Feng et al. 2018.)

There are three different types of PCD reactors, which utilize catalytic materials for enhanced pollution control: Continuous operation in plasma catalyst (CIPC) system, sequential operation in plasma catalyst (SIPC) system and post plasma catalyst (PPC) system. Catalytic material can be in the form of powder, beads, or a simple coating. When the catalyst is placed to the discharge zone of PCD reactor, it is considered a single-stage system or in-plasma catalysis (IPC). CIPC and SIPC are single-stage systems because the catalysts are placed in the PCD reactor. In such systems, catalyst and plasma interact with the fluid simultaneously. In a PPC system the catalyst is placed after the PCD reactor. Catalytic substances include zeolites, activated carbon, noble metals and metal oxides. Byproducts and unreacted pollutants as well as ozone created in the PCD reactor react with catalyst which increases the removal of pollutants. (Feng et al. 2018.)

2.3.2 Photocatalysis in gaseous phase

Photocatalytic oxidation typically uses semiconductor nanoparticles as photocatalysts and ultraviolet light to convert pollutants into harmless substances such as water vapor and carbon dioxide (Mo et al. 2009). Titanium dioxide (TiO_2) along with zinc oxide (ZnO) are two of the most commonly used catalytic materials due to wide energy band-gap, although a wide variety of materials have been employed as catalysts for PCO (Boyjoo et al. 2017). TiO_2 has been widely adopted as it is inexpensive, chemically stable, and highly active. It has two crystal forms anatase and rutile having energy band-gaps 3.23 V and 3.02 V, respectively (Mo et al. 2009).

In the activation of the catalytic surface positively charged holes and vacant electrons form under ultraviolet irradiation. Compounds that are adsorbed to the surface can be reduced by the electrons or oxidized by the electron holes. Strong oxidants such as hydroxyl radicals are photogenerated from water vapor on the surface of the catalyst, increasing catalytic activity of the process (Mo et al. 2009).

Several factors influence the photocatalytic reaction rate including UV light wavelength and intensity, pollutant concentration, humidity, temperature, surface velocity, residence time and catalyst loading. UV light wavelength should be less than 380 nm to activate TiO_2 catalyst. Increasing light intensity can increase the reaction rate. Sunlight intensity is about 1-2 $mW \cdot cm^{-2}$ for wavelengths below 350 and 400 nm, respectively (Mo et al. 2009).

Humidity affects the photocatalysis as water vapor reacts with the positively charged holes. This reaction creates hydroxyl radicals which in turn facilitate the oxidation of pollutants. Excessive water vapor will in turn inhibit the decomposition of pollutants due to competition for adsorption sites. It is possible to find experimentally an optimal concentration of water vapour for various pollutants, where the competitive adsorption is low, but the generation of hydroxyl radicals facilitates pollutant oxidation (Mo et al. 2009).

Increasing temperature has two major impacts on the photocatalytic process. Temperature affects the coverage of pollutants on the photocatalyst surface so that with increasing temperature the pollutant coverage progressively decreases. If mass transfer is the limiting reaction parameter, increasing temperature will decrease the reaction rate. However, in cases where reaction rate rather than mass transfer is the limiting factor for PCO, increasing temperature will increase the overall reaction rate. An optimal temperature range can be found for different pollutants (Mo et al. 2009).

Photocatalyst activity decreases over time due to the deactivation of active catalyst sites of the reaction surface. Active sites may be blocked when reaction residues are adsorbed to the catalyst or the pores may be blocked by small solid particles in the gas stream, referred to as fouling (Mo et al. 2009).

3. MATERIALS AND METHODS

3.1 Reagents and chemicals

All used reagents were of analytical grade and used without further purification. Milli-Q ultrapure water was used for preparing toluene reference solutions. Other aqueous solutions were prepared using distilled water. Toluene (C_7H_6, ≥99.9%) and sodium hydroxide (NaOH, ≥98.0%), were purchased from Sigma-Aldrich. Sodium sulfate anhydrous (Na_2SO_4, 99.3%) was purchased from LachNer. Dichloromethane (CH_2Cl_2 ≥ 99.8%) was purchased from Fisher Scientific. Methanol for HPLC (CH_3OH ≥ 99.9%) was purchased from Honeywell.

3.2 Air pollution

The toluene vaporization setup was operated in continuous mode (figure 1). For the generation of polluted air, toluene was vaporized using a bubble column. The Eco Air Pump PA200 (Jecod Co. Ltd., People's Republic of China) with flow rate varying from 1 to 6 m^3h^{-1} fed air through the reactors. A bypass controlled by a valve directed a 0.1 $L\cdot min^{-1}$ part of the main air flow through a bubble column (H = 700 mm; d_i = 50 mm) filled with liquid toluene (500 ml). The air flowing through column saturated with toluene vapor and was mixed with the main air flow. Toluene concentration in the air was determined with air/bypass flow ratio. Bypass and air flow rates were measured by rotameters. Air was pumped first to PCD reactor and the to PCO reactor. All experiments were performed at the room temperature, 22°C, atmospheric pressure, and relative humidity of 30±3 %.

Figure 3. Experimental laboratory setup.

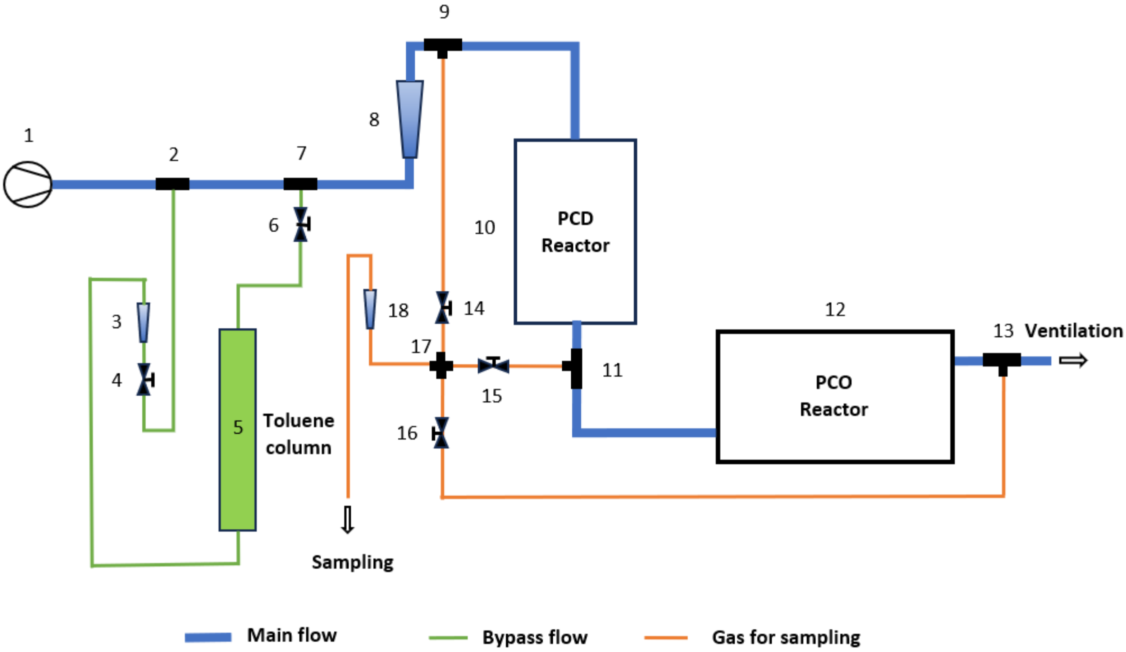

Figure 4. Experimental setup flow chart: 1 – Air pump, 2 – Flow divider, 3 – Rotameter, 4 – Control valve, 5 – Toluene column, 6 – Control valve, 7 – Flow divider, 8 – Main rotameter, 9 – Sampling tube connector, 10 – PCD reactor, 11 – Sampling tube connector, 12 – PCO reactor, 13 – Sampling tube connector, 14 – Sampling valve, 15 – Sampling valve, 16 – Sampling valve, 17 – Tube connector, 18 – Sample rotameter.

3.3 Reactors

3.3.1 Pulsed corona discharge reactor

The PCD setup (Flowrox Oy, Finland) (figure 5) consists of a 154 L reactor with a 40 L storage tank, a pulse generator, and a circulation pump (Iwaki Co. Ltd., Japan).

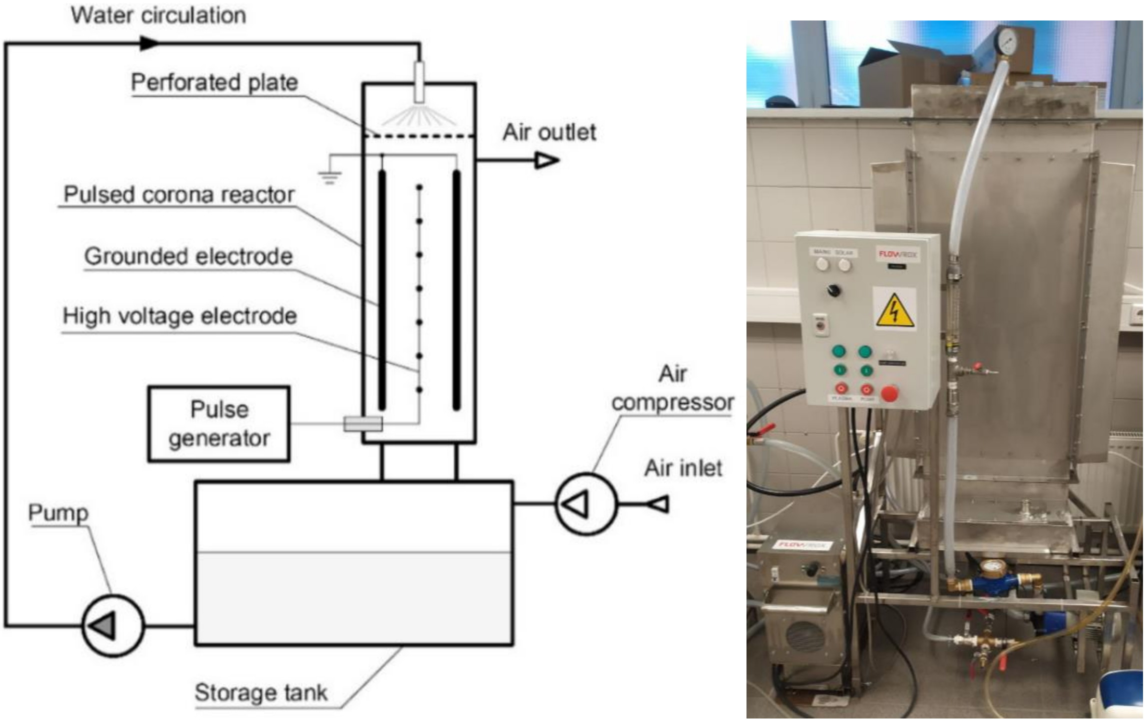

Figure 5. PCD reactor scheme (left) and image of the reactor (right).

A perforated plate with 51 holes of 1 mm diameter was used to spread aqueous solution into the plasma zone. High voltage pulses (20 kV) were applied between two horizontal voltage electrodes constructed of 0.55 mm diameter stainless-steel wire with a total length of 20 m and two vertical grounded stainless-steel parallel plates having repetition frequency varied between 100–800 pps producing 12.5–100 W of output power.

Two recirculation water flow rates were used: 9.0 $L \cdot min^{-1}$ and 2.6 $L \cdot min^{-1}$. pH of recirculation water was adjusted either with acidic (5 M H_2SO_4) or alkaline solution (10 M NaOH) and determined using a digital pH meter (S220 Mettler Toledo, Switzerland).

3.3.2 Photocatalytic oxidation reactor

The plug flow PCO reactor is flat bedded with a transparent cover (2 mm polyethylene terephthalate, PET) sealing in the gas passing through a maze-like chamber where glass plates covered with TiO_2 lay on the chamber floor as shown in Figure 6. Twenty UV-A lamps provide radiation withing 315–400 nm wavelength and 119 $W \cdot m^{-2}$ intensity at the surface of the photocatalyst.

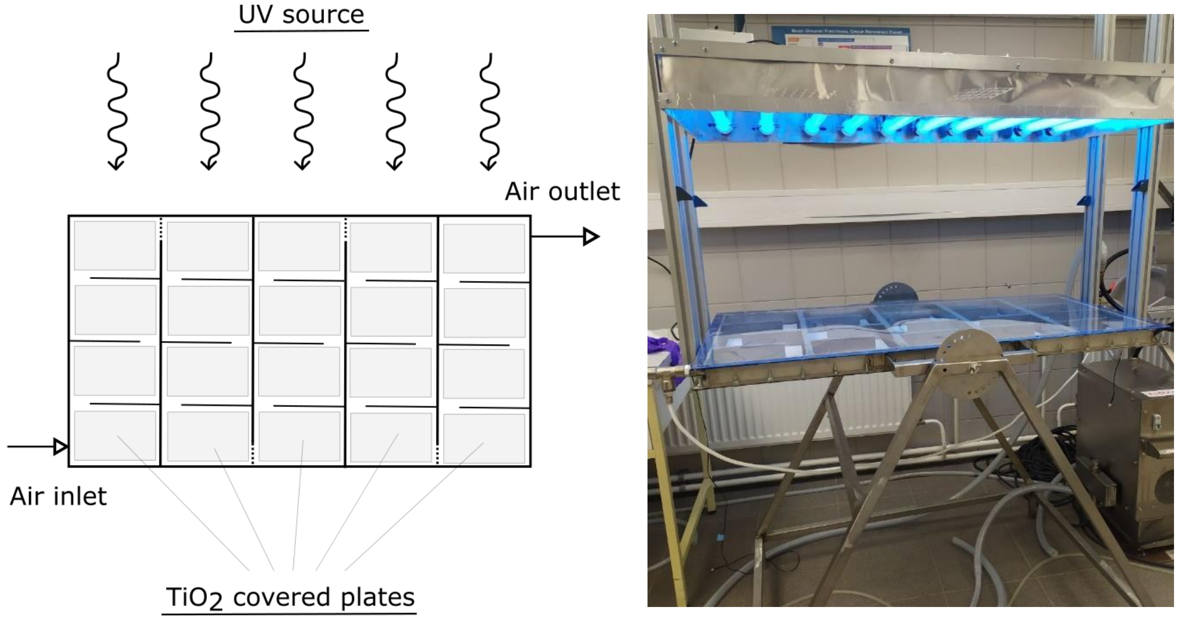

Figure 6. Photocatalytic oxidation reactor illustration (left) and image (right).

Entering the PCO reactor, polluted air flows through a series of chambers encountering the surface of the photocatalyst. The dimensions (L, W, H) of the reactor are as follows: 996 mm, 534 mm, and 40 mm, respectively. The total volume of the reactor is 21.3 liters. The reactor is divided into five sections sized 4.26 L with stainless-steel plates with holes in the end of each section providing diagonal air flow along the sections. The air flow rate in the reactor was 6.0 m^3h^{-1}, which corresponds to a residence time of 13 s.

For ozone conversion experiments in the PCO reactor ozone was produced with ozone generator. The initial concentration of ozone for the experiments was 22.6 ppm. Light irradiation varied between 29 and 119 $W \cdot m^{-2}$ and gas flow rate between 1.0–6.0 m^3h^{-1}, which corresponds to residence times of 13–66 seconds.

3.4 Determination of toluene

3.4.1 Gaseous phase

The residual toluene concentration in air was assessed using Fourier transform infrared spectroscopy (FTIR, Interspec 200-X, Estonia). Gaseous samples were collected in the Specac Atmos 20.0 m 3.68 L gas cell and analyzed in the 500–4000 cm^{-1} wavelength range. The spectrum was taken in each gaseous sample and analyzed using essential FT-IR software (Operant LLC) equipped with a quantitative database (FDM, HiRes VPFTIR for Quant).

The concentration of O_3 was measured using ozone analyzer (MP-6060, Anseros Klaus Nonnenmacher GmbH, Germany).

3.4.2 Liquid phase

The concentration of toluene in liquid phase was determined using a high-performance liquid chromatography (HPLC, Shimadzu) equipped with a PDA detector and a C18 column (Luna Omega, 100 Å pore size, 5 µm particle size, 150 mm length, and 2.1 mm inner diameter). Eluent flow rate was set to 0.2 $mL \cdot min^{-1}$ throughout the 20-minute sample run. Isocratic elution was achieved using 70 % ultrapure water and 30 % methanol. All the samples were measured at the wavelength of 261 nm which corresponds to maximal absorption by toluene (figure 7). UV-Vis spectra was measured using spectrophotometer (Thermo Fisher Scientific Inc., Genesys 10S UV-Vis).

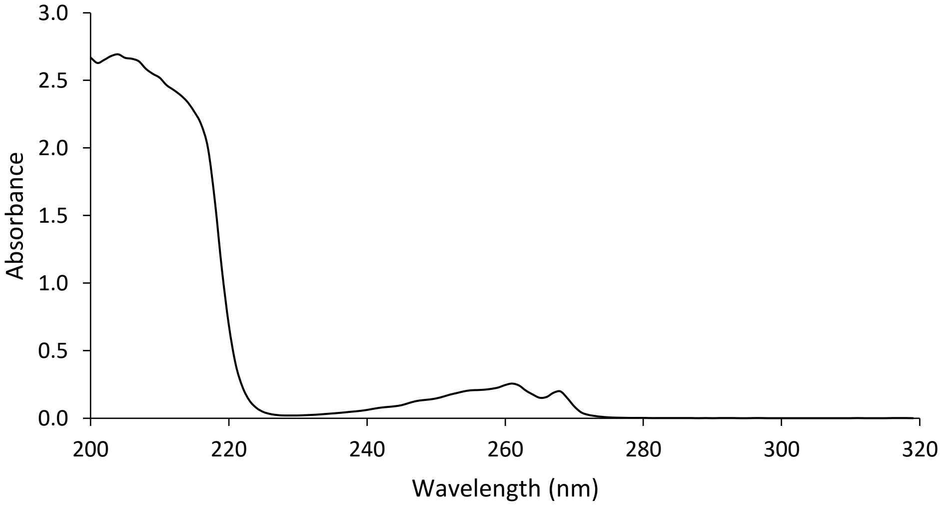

Figure 7. UV-Vis absorbance spectrum of toluene in water. Toluene concentration was 100 $mg \cdot L^{-1}$.

The method was calibrated by toluene standard solutions with the concentration varied between 1–20 mg·L^{-1} (figure 8).

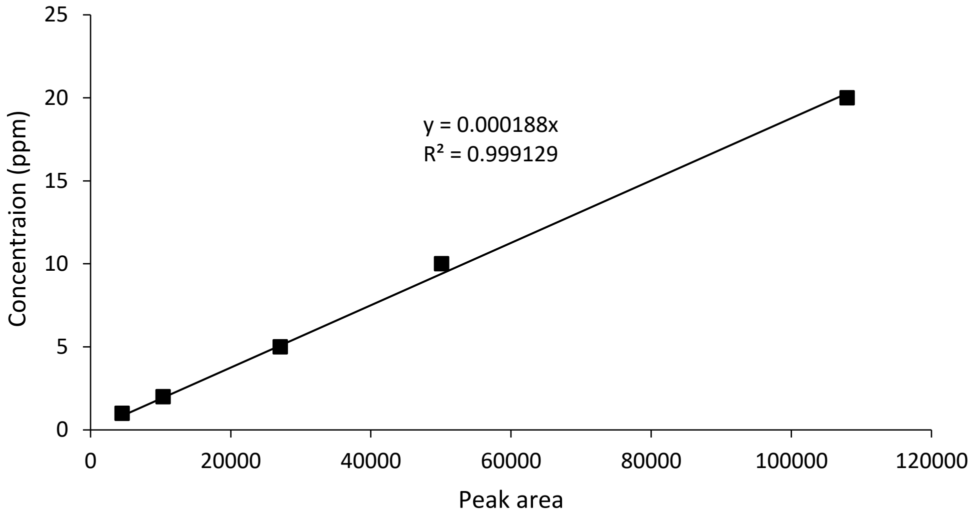

Figure 8. Toluene calibration curve for HPLC.

All measurements were repeated to ensure that the standard deviation was less than 5%.

4. RESULTS AND DISCUSSION

4.1 Degradation of toluene and ozone in gaseous phase

The treatment of polluted air includes the gaseous reactions in PCD reactor as well as the post treatment of reactor gases with PCO reactor. Concentration of toluene in inlet and outlet of PCD varied between 39–54 ppm and 11–36 ppm, respectively. Figure 9 compares removal efficiency of the PCD reactor with the pulse frequency. At the beginning removal efficiency increases by 15 % from 100 pps to 200 pps. However, less increase in removal efficiency is gained with rising pulse frequencies illustrated by the flattening curve in figure 9.

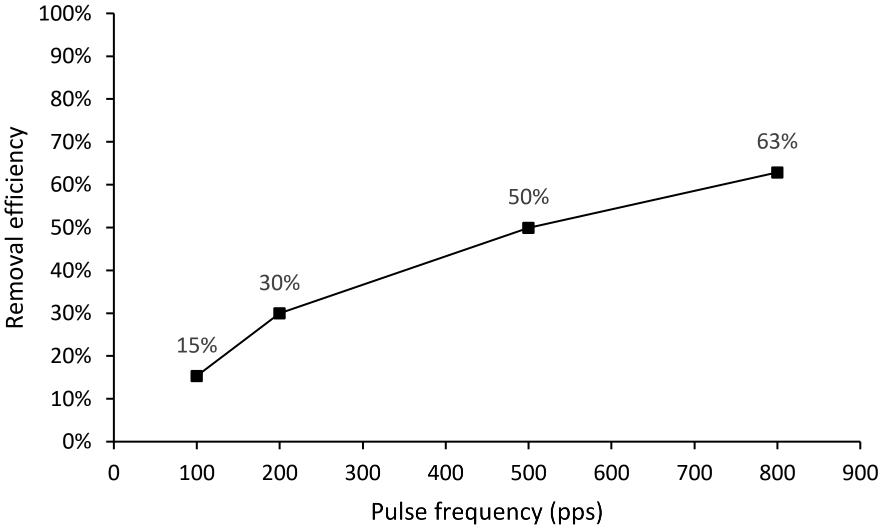

Figure 9. Toluene removal efficiency from air after 30 minutes of PCD reactor operation.

Residual toluene as well as ozone generated in PCD reactor remain in the treated air and thus requires additional treatment. Gas mixture was treated with photocatalytic oxidation reactor employing TiO_2 as a photocatalyst and UV-A lamps.

Following PCD, the degradation of residual toluene was accomplished in PCO reactor. Toluene concentrations of 22.6 ppm and 11.6 ppm before PCO decreased to 15.0 ppm and 9.2 ppm after the photocatalytic treatment. Thus, 27.2 % of toluene was removed.

The mechanism of toluene degradation over various photocatalysts has been studied by several authors (Zhang et al. 2023, Zhou et al 2023, Hernández-Alonso et al. 2011). Hernández-Alonso et al. (2011) studied photocatalytic oxidation of methylcyclohexane and toluene on TiO_2-ZrO_2 thin films. They observed deactivation of photocatalyst by toluene oxidation products. Benzoate species, which were identified as the main partial oxidation products of toluene, tend to be adsorbed to the surface of the catalyst vertically, leaving aromatic rings isolated from the photoactive sites. In our process no deactivation was observed. Altof et al. (2023) found out that ozone maintained the photocatalyst activity by cleaning the photocatalytic plates from oxidation products of toluene, which was also observed in given study. Thus, it could be concluded that the presence of ozone supports photocatalytic oxidation of toluene by prevention of byproducts adsorption on the photocatalytic sites.

Based on the experience of previous studies the degradation pathway and expected byproducts of toluene could be proposed. Zhou et al. (2023) studied toluene oxidation over CeO_2 and $Ce_{0.8}Mn_{0.2}O_2$ photocatalysts. They observed that doping CeO_2 catalysts with Mn enhances the absorption of benzene ring and promoted the activation of ring-opening reactions. With simple CeO_2 catalyst toluene oxidation resulted in formic acid and benzene products (figure 10), which could further be oxidized to acetone, acetic acid and finally CO_2 and H_2O. With $Ce_{0.8}Mn_{0.2}O_2$ catalyst the aromatic ring was oxidized resulting in methanol and sorbic acid as oxidation products (figure 11), which were further oxidised to several oxidation products.

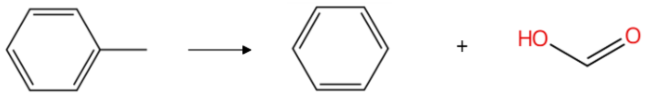

Figure 10. Toluene oxidation over CeO_2 catalyst to benzene and formic acid.

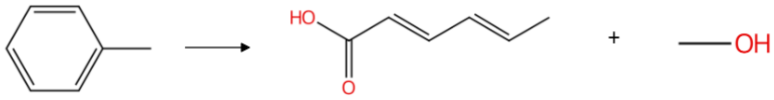

Figure 11. Toluene oxidation over $Ce_{0.8}Mn_{0.2}O_2$ catalyst to sorbic acid and methanol.

Zhang et al. (2023) proposed toluene oxidation path where the C-H bonds of methyl groups are first cracked yielding benzyl species. Unstable oxidation products oxidize further to benzyl alcohol, benzaldehyde, and benzoic acid, which finally leads to aromatic ring opening and ultimately generates CO_2 and H_2O (figure 12).

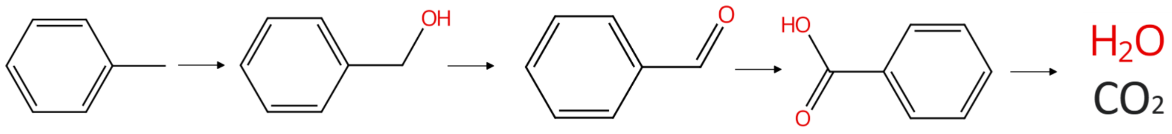

Figure 12. Toluene oxidation over CuCeZr/T catalyst to benzyl alcohol, benzaldehyde, benzoic acid, and finally to CO_2 and H_2O.

Several oxidants are formed during PCD treatment, including ozone, hydroxyl radical, hydrogen peroxide, atomic oxygen and singlet oxygen (Ajo et al. 2017). Ozone O_3 and hydroxyl radical •OH are strong oxidants with oxidizing potentials 2.07 V and 2.33 V, consequently (Panorel 2013). They are also the most abundant oxidants generated in PCD reactor (Ajo et al. 2017). Ozone is generated in PCD reactor as a result of air oxygen ionization caused by non-thermal plasma. Hydroxyl radical lifetime in matrices does not exceed milliseconds, whereas ozone is considerably more stable, which comprises an issue, because residual ozone is present in treated air. Figure 13 demonstrates ozone concentration curves measured by ozone analyser. As it can be seen from the graph, ozone is formed immediately after ignition of the plasma achieving the concentration plateau after ca 3 min. Ozone concentration in reactor exhaust increases from 40 ppm to 235 ppm proportionally with increasing pulse frequency.

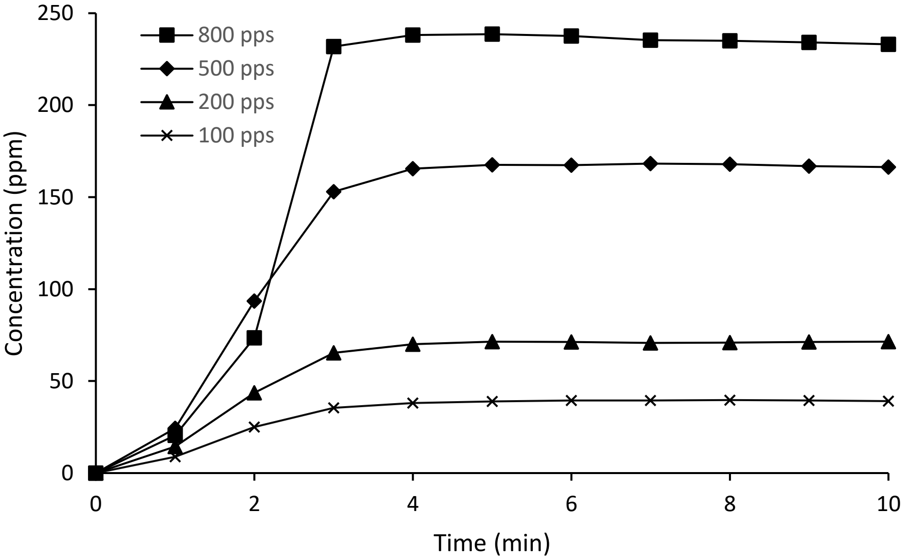

Figure 13. Ozone concentration in PCD reactor during the experiments with various pulse frequency from 100 to 800 pps.

Ozone is considered a pollutant and needs to be removed for example by PCO. The effect of PCO in ozone conversion is illustrated in figure 14 which demonstrates the immediate ozone concentration change when gas mixture travels through PCO reactor. The PCD process generates ozone at concentration of 70 ppm (figure 13). After 10 minutes the air flow was directed to photocatalytic reactor where degradation of ozone took place. New equilibrium at approximately 55 ppm was reached. As a result, around 23 % of ozone conversion was achieved by the photocatalytic reactor with UV-A intensity of 65 W·m^{-2} and residence time of about 13 seconds. With a larger catalyst surface or lower flow rate a higher ozone conversion could be reached.

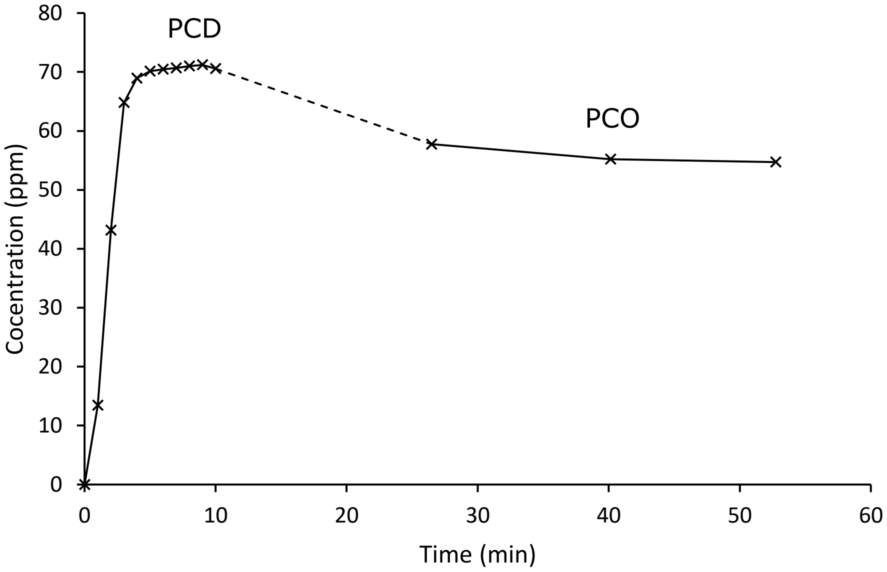

Figure 14. Ozone concentration decrease in PCO reactor after air treatment with PCD at 200 pps.

Experiments on the effect of residence time and radiation intensity on ozone degradation were also made. Degradation of ozone in air with various irradiances and residence times may be seen in figure 15. A linear trend appears in all irradiation levels as the residence time increases. Increasing the irradiation of photocatalyst leads to better ozone conversion to some extent. This indicates that ozone conversion rate is limited by reaction kinetics with the photocatalyst.

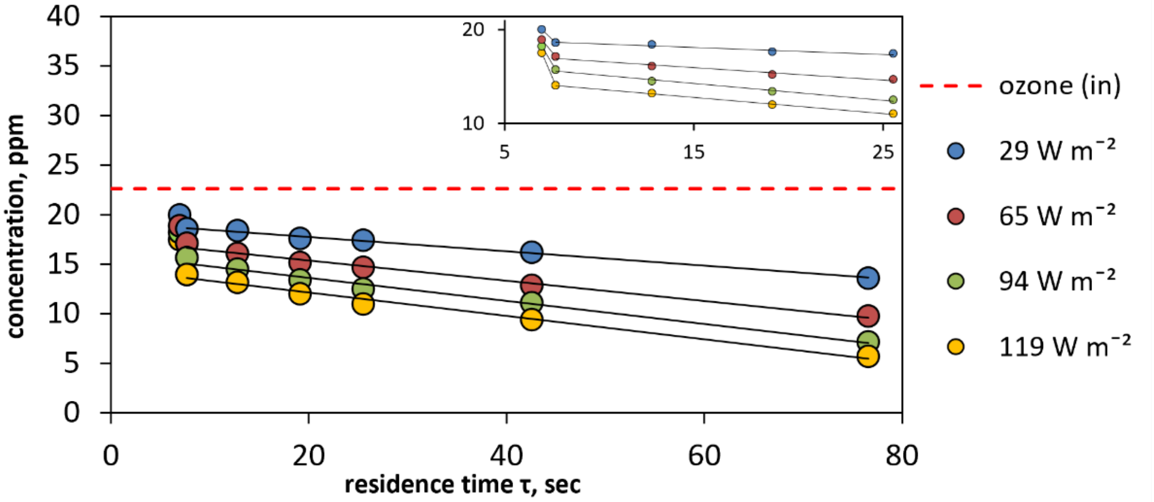

Figure 15. Photocatalytic degradation of ozone using various UV intensities and residence times (Altof et al. 2023).

The linear trend of ozone degradation could be explained in terms of mass balance in an ideal plug flow reactor as follows (Eq. 6):

$$\text{Accumulation} = \text{inflow} - \text{outflow} + \text{generation} \tag{5}$$

$$\frac{\partial C}{\partial t}\Delta V = QC|_{L} - QC|_{L+\Delta L} + r_c \Delta V \tag{6}$$

where ΔV – differential volume element of the reactor,

Q – volumetric flow rate,

C – concentration of a substrate in air

L – length of flow path,

r_c – reaction rate for photocatalysis.

Equation 6 can be transformed and rewritten to Eq. 7:

$$\frac{\partial C}{\partial t} = -\frac{Q}{A}\frac{\partial C}{\partial L} + r_c \tag{7}$$

where A is the surface area of the reactor. In PCO, the reaction rate r_c is commonly modelled with Langmuir-Hinshelwood (LH) kinetics of heterogeneous catalysis (Eq. 8) (Ollis 2005).

$$r_c = -\frac{k_r KC}{1 + KC} \tag{8}$$

where k_r – limiting rate constant of the reaction,

K – absorption equilibrium constant,

C – substrate concentration.

LH reaction rate in equation 8 and steady-state conditions $\partial C/\partial t = 0$ in equation 7 can be assumed to write mass balance as follows (Eq. 9):

$$\frac{Q}{A}\frac{dC}{dL} = -\frac{k_r KC}{1 + KC} \tag{9}$$

When $KC << 1$, first order kinetics emerge, whereas at $KC >> 1$ zero order reaction kinetics can be observed at surface saturation. This suggests that all reaction sites are occupied by the substrate and the LH reaction rate can be approximated by a constant k_{obs} (Eq. 10).

$$\frac{Q}{A}\frac{dC}{dL} = -k_{obs} \tag{10}$$

Thus, linear dependence between the residence time and concentration can be gained (Eq. 11) by integrating equation 10 between the concentration limits C_0 and C which correspond to path lengths L = 0 and L = L of plug flow reactor.

$$C = C_0 - \frac{A}{Q} \cdot L \cdot k_{obs} = C_0 - \tau \cdot k_{obs} \qquad (11)$$

Equation 11 corresponds to pseudo-zero order reaction process, where the initial concentration of substrate has no influence on the reaction kinetics. Biard et al. (2007) made the same observation with their plug flow PCO reactor. Gong et al. (2017) studied ozone degradation in photocatalytic reactors with TiO_2 catalysts and showed that there is also a linear dependence on ozone degradation with photocatalyst coating area and the gas flow rate.

However, figure 15 shows some deviation from linearity at residence time less than 7 seconds (figure 15, see inset). The cross sections of linear paths according to equation 11 are below the initial concentration of 22.6 ppm. This could be explained with a diffusion-controlled process at short residence time, where at extremely high gas flow rate reaction rate becomes limited by the ozone transport to the active sites of the catalyst.

4.2 Behaviour of toluene in the recirculation water

Although the main objective was to reduce toluene concentration in gaseous phase, toluene oxidation in aqueous phase requires also attention. Water plays an important role in PCD process because it serves as a source for formation of hydroxyl radicals in the system. Hydroxyl radicals are mainly produced in PCD reactor when free electrons collide with water according to equation 12 (Ono and Oda 2003).

$$\mathrm{H_2O} + e^- \rightarrow \bullet\,\mathrm{OH} + \mathrm{H} + e^- \tag{12}$$

Ajo et al. (2017) suggested that hydroxyl radicals need H scavengers to prevent immediate recombination of •OH and H back to H_2O. Gaseous oxygen acts as an effective scavenger which makes gas-phase suitable environment for •OH radical formation. In gas phase, hydroxyl radicals are generated from water vapour. Although •OH radicals are also generated in water, their lifetime is substantially shorter than in gas-phase (Kanazawa et al. 2011). Due to short lifetime, •OH radicals in water are unlikely to cross the interfacial boundary of water droplets and can only react with dissolved compounds (Ajo et al. 2017).

4.2.1 Toluene saturation in water

Specific mass-transfer rate of toluene into liquid is of great interest, because it affects the overall efficiency of the process. Considering that the degradation of toluene could occur in aqueous phase as well, its absorption to water is of high interest. Thus, better mass-transfer between gas and liquid phase can improve the performance of PCD reactor. Toluene oxidation in water is discussed in detail in the next section (Section 4.2.2).

Saturation of water with toluene and more generally the mass transfer from one phase to another is driven by concentration difference between the two phases. Separating interface between phases causes resistance for mass transfer, which leads to a concentration gradient in each phase. Molar flux (N) is used to describe the transition of molecules between phases. It is proportional to concentration gradient between phases and depends on a constant k – mass transfer coefficient. Molar flux into liquid phase is described by equation 13 (Gottschalk et al. 2000).

$$N = k_L(c_{Li} - c_L) \tag{13}$$

where N – molar flux into one phase,

k_L – mass-transfer coefficient for liquid film,

C_{Li} – liquid concentration in equilibrium with the gas concentration at the interface,

C_L – concentration of compound in the bulk liquid.

Similar equation can be written for the gaseous phase to receive the balance between the two phases. Mass transfer is presented graphically in figure 16.

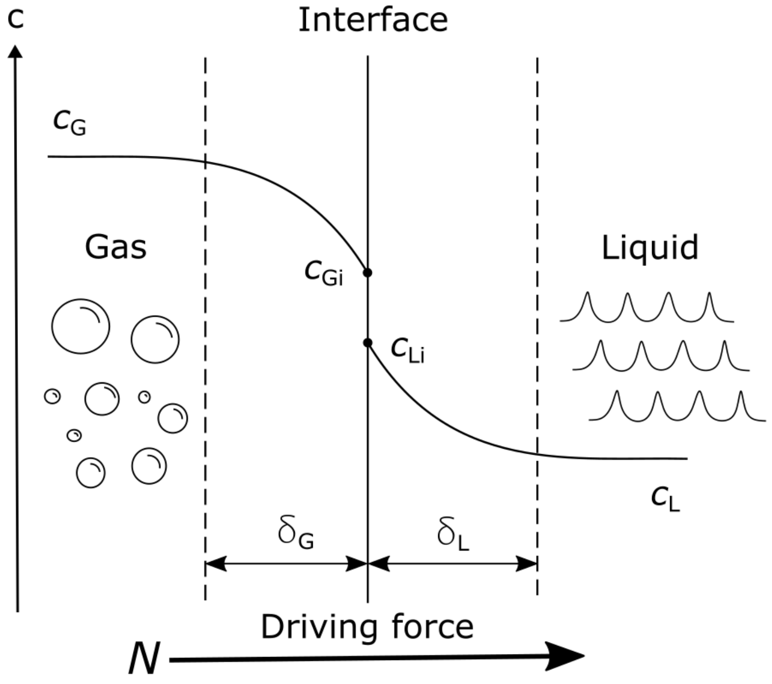

Figure 16. Mass transfer between gaseous and liquid phase (Gottschalk et al. 2000, edited by Daniel Teittinen). c_G – concentration in gas phase, c_{Gi} – concentration at the gas-liquid interface, c_{Li} – concentration at the liquid-gas interface, c_L – concentration in liquid phase, δ_G – laminar gas film width, δ_L – laminar liquid film width, N – molar flux.

Current mass transfer theory suggests that a laminar film develops at gas-liquid interface. This laminar film causes most of the resistance to mass transfer as shown in figure 16. Concentration curve drops rapidly in the laminar film in gas and liquid sides. Resistance of the bulk fluid is negligible. Concentrations c_{Gi} and c_{Li} immediately adjacent to the interface are unequal. Concentration difference at the interface is determined by the thermodynamic equilibrium distribution between phases. (Gottschalk et al. 2000.)

Specific mass-transfer rate of gas to liquid at any given point of time can be determined if the interfacial surface area and equilibrium concentration is known (Eq. 14) (Gottschalk et al. 2000).

$$m = K_L a(c_L^* . c_L) \tag{14}$$

where m – specific mass-transfer rate to liquid,

K_L – overall mass-transfer coefficient,

$a = A/V_L$ – volumetric interfacial surface area,

c_L^* – equilibrium liquid concentration,

c_L – bulk concentration in liquid.

Equilibrium distribution between gas and liquid phases is reached when the concentration becomes constant in liquid. In other words, the net flow over gas-liquid interface is zero for the compound of interest. The saturation concentration for toluene can be predicted using Henry's law (Eq. 15).

$$c_m^* = \frac{P_i}{H} \tag{15}$$

where c_m^* – molar concentration of toluene in water, $kg \cdot mol^{-1}$,

P_i – partial pressure of toluene in air, bar,

H – Henry's constant.

From the literature can be found that Henry's constant for toluene in normal temperature and pressure (NTP) conditions is 0.173 $mol \cdot (kg \cdot bar)^{-1}$ (NIST 2023). When the concentration of toluene in air is known, partial pressure of toluene and the molar concentration in saturated water can be calculated.

Determining the volumetric interfacial surface area (equation 14) is more difficult. Some estimations could be made based on the volume of PCD reactor and flow rate of gas and circulation water, but determining the geometry of water droplets and gas flow conditions in the PCD reactor is out of scope for this thesis. Instead of measuring the interfacial area separately, it can be lumped together with the overall mass transfer coefficient K_L and measured as one parameter K_La (Gottschalk et al 2000).

Gottschalk et al. (2000) proposed a batch process mass balance for liquid phase at nonsteady-state. Concentration of toluene can be presented over time with the following equation 16.

$$\frac{dc_L}{dt} = k_L a \cdot (c_L^* - c_L) - r_L \tag{16}$$

where k_La – mass-transfer coefficient,

c_L^* – equilibrium concentration corresponding to influent gas,

c_L – dissolved concentration of toluene in water,

r_L – reaction coefficient, which accounts for the reduction of dissolved toluene due to chemical reactions.

In a simple saturation experiment without the presence of non-thermal plasma $r_L = 0$. By solving differential equation 16 in the concentrations range C_L to C_L^* and time from 0 to t the equation takes form (Eq. 17):

$$-ln\left(1-\frac{c_L^*}{c_L}\right)=k_L a\cdot t \tag{17}$$

Figure 17a demonstrates the saturation profiles of toluene in water. The mass-transfer coefficient k_La could be found by the slope of the linear curves (figure 17b). k_La follows well the measured toluene concentrations in water. With lower water recirculation flow rate of 2.6 L·min^{-1} the linearized curve has lower slope than with 9.0 L·min^{-1} indicating lower mass-transfer rate. Same observation can be made based on the saturation curves in figure 17a. Saturation to 95 % with recirculation flow rates 9.0 L·min^{-1} and 2.6 L·min^{-1} takes 5.7 and 10.9 minutes, consequently. Less contact between incoming air and recirculation water with lower flow rate leads correspondingly to lower mass-transfer between the phases whereas at high recirculation flow rate toluene has more contact with water droplets which makes the saturation faster.

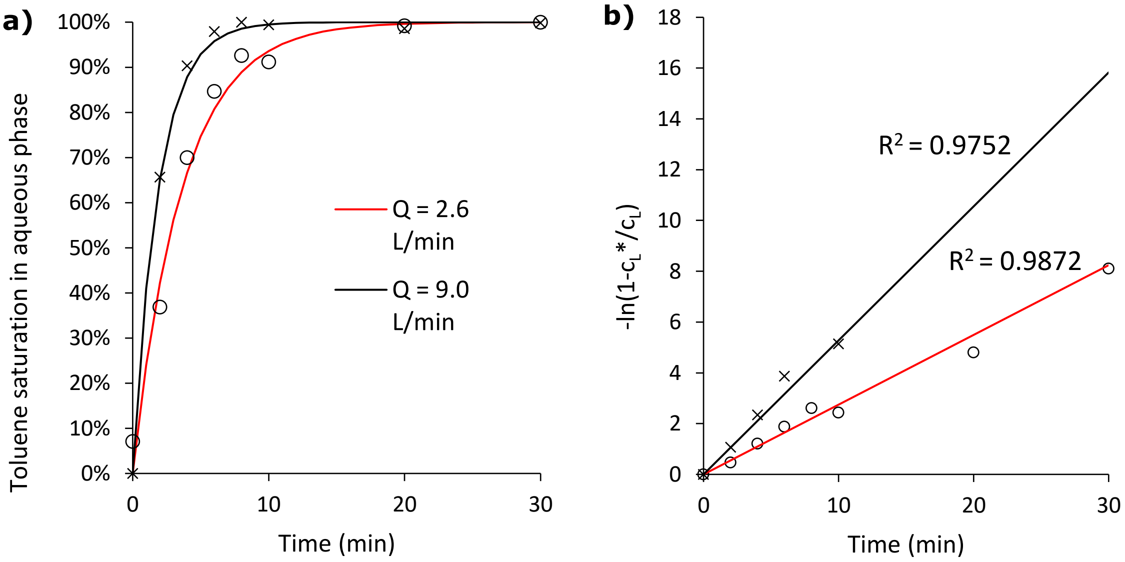

Figure 17. Saturation curves of toluene in water (a) and their linearized forms (b). Toluene concentration in air is 30 ppm on average. 100 % saturation corresponds to 1.7 ppm aqueous toluene concentration.

Chemical reactions during PCD reactor operation affect toluene mass transfer to water. Mass balance calculations become more complex due to simultaneous degradation of toluene and possible enhanced mass-transfer due to chemical reactions, known as chemisorption, may occur. Two parameters should be considered for the optimal mass transfer rate and the process equilibrium concentration of toluene in water during PCD operation: energy consumption of the circulation water pump and the amount of degraded toluene in gaseous phase.

4.2.2 Oxidation of toluene in water

Toluene concentration was measured in circulation water over 30 minutes experiment (figure 18). Prior to the PCD reactor start up recirculation water had been saturated with toluene. Toluene concentration in circulation water decreases sharply after 2 minutes of operation, with 47 % reduction in concentration at 800 pps. After 10 minutes toluene aqueous concentrations stabilized reaching equilibrium. It could be concluded that at the equilibrium state the absorption of toluene to water is equalized with the degradation.

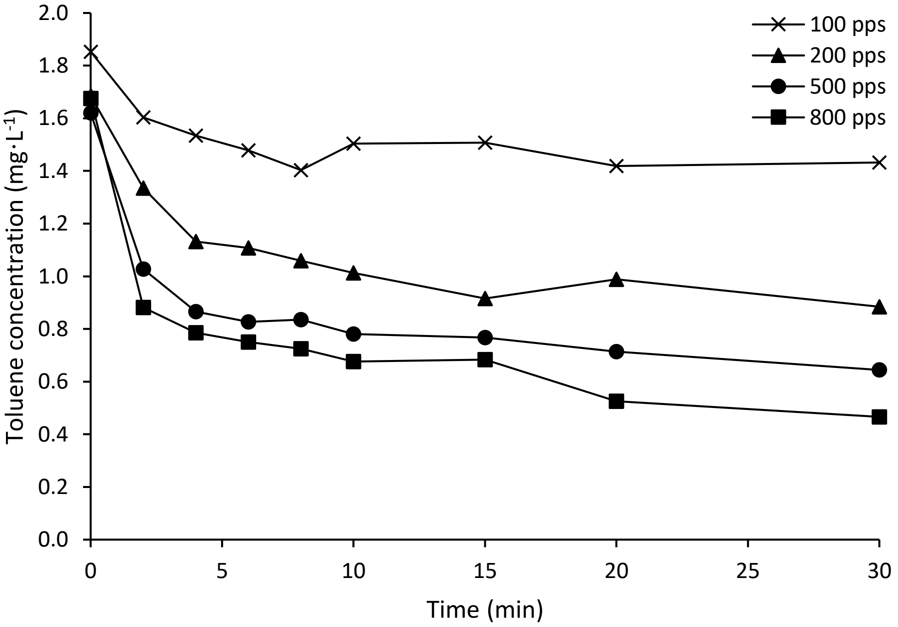

Figure 18. Toluene concentration decrease in circulation water of PCD reactor.

Figure 19 shows toluene aqueous concentrations at equilibrium. It is reasonable to assume that lower pulse frequency results in less effective degradation of toluene in aqueous phase. With lower pulse frequency (100 pps), concentration in water drops only slightly (22.7 %), whereas 800 pps resulted in more effective removal of toluene from water (72.0 %). Some concentration remains even at the highest pps indicating the toluene entering to circulation water despite the oxidation processes taking place. According to equation 16 the presence of chemical reaction increases the molar flux by modulus. Thus, a faster toluene degradation in water may also increase the mass-transfer of toluene from gas to water.

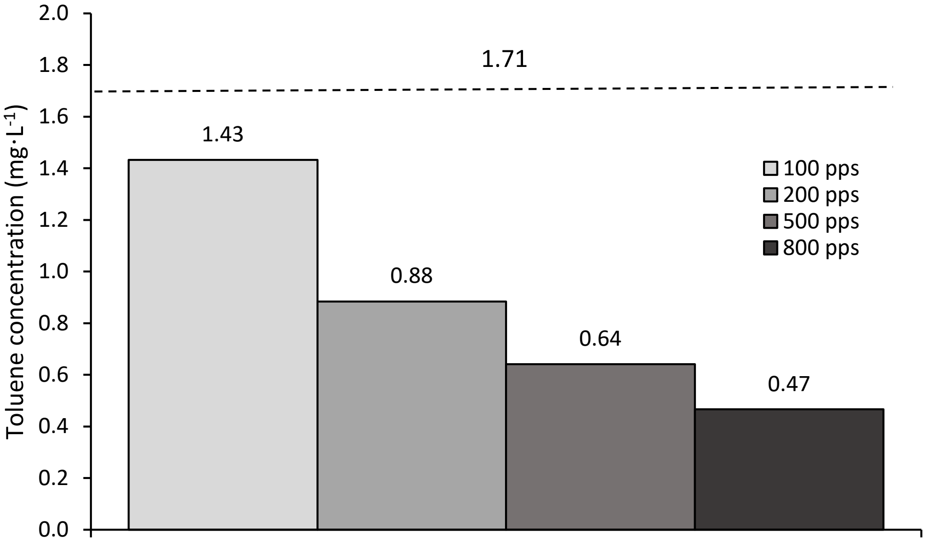

Figure 19. Toluene concentration in PCD reactor circulation water after 30 minutes of operation. Initial concentration shown as a reference.

4.3 Efficiency and operational costs

Energy efficiency of the PCD reactor is calculated using equation 18.

$$E = \frac{\Delta C \cdot Q}{P} \tag{18}$$

where E – energy efficiency, g·kWh^{-1},

ΔC – concentration difference between inlet and outlet of PCD reactor, g·m^{-3},

Q – volumetric flow rate, 6.0 m^{3}·h^{-1},

P – reactor power, W.

Energy efficiencies of toluene removal are presented in table 2. Highest energy efficiency is obtained by 200 pps with 12.70 grams of toluene removed per kWh. Figure 20 shows how energy efficiency decreases when more power is applied to PCD. An optimal pulse frequency should be applied to reach the best energy efficiency.

Table 2. Toluene removal energy efficiency with four pulse frequencies.

Pulse frequency (pps)	ΔC (g·m^{3})	P (W)	E (g·kWh^{-1})
100	0.025	12.5	12.06
200	0.053	25	12.70
500	0.082	62.5	7.86
800	0.107	100	6.44

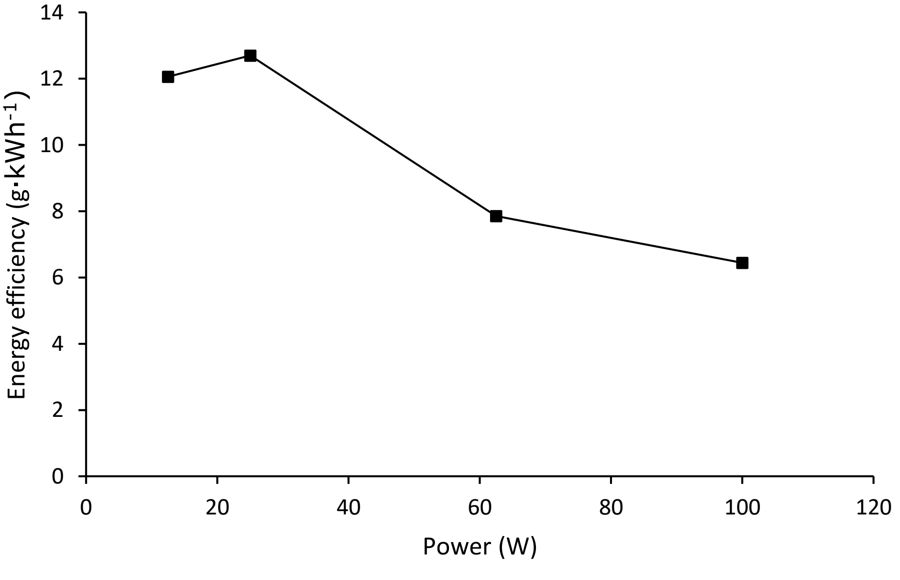

Figure 20. Toluene removal energy efficiency as a function of PCD power.

It is possible to calculate the price for toluene removal with the current experimental equipment. Tables 3 and 4 show the price for removal of toluene in PCD and PCO, and conversion of ozone in PCO. Electricity price is assumed to be 12 cents per kWh.

Table 3. Price for toluene removal.

Frequency	Removal efficiency (%)			Energy efficiency (g·kWh^{-1})			Price
(pps)	PCD	PCO	Total	PCD	PCO	Total	(€·g^{-1})
100	15%	27%	38%	12.06	0.75	12.81	0.009
200	30%	27%	49%	12.70	0.67	13.37	0.009
500	50%	27%	64%	7.86	0.44	8.30	0.014
800	63%	27%	73%	6.44	0.34	6.78	0.018

Table 4. Price for ozone conversion.

Frequency (pps)	Resultant ozone concentration (ppm)	Removal Efficiency (%) PCO	Energy efficiency (g·kWh^{-1})	Price (€·g^{-1})
100	40	23%	0.75	0.16
200	71	23%	0.67	0.18
500	168	23%	0.44	0.27
800	235	23%	0.34	0.35

Based on the results in tables 3 and 4 it could be concluded that low pulse frequencies are more energy efficient, whereas higher pulse frequencies surpass in terms of compound’s removal. In the current PCD and PCO equipment, ozone conversion is more energy demanding compared to toluene removal. Currently used PCD reactor is able to remove high toluene concentrations producing however ozone which requires also removal. Depending on the type of PCD application, the process should be optimized, e.g. compact solutions for indoor air cleaning with less ozone production or industrial applications for removing high toluene concentrations.

5. CONCLUSIONS

In this master’s thesis the degradation of toluene was examined implementing PCD process combined with PCO as a post treatment method. The oxidation reactions most likely take place on the surface of water droplets where oxygen in air is available as an H scavenger to prevent recombination of hydroxyl radicals. Circulation water plays thus a crucial role in the oxidation process of toluene in PCD reactor. The saturation of toluene in circulation water was found to follow convective mass-transfer equation (13). The measured data points fit well to the theoretical background. During PCD operation toluene concentration in water decreased with rising pulse frequency, but faster toluene degradation in water seems to accelerate the mass-transfer of toluene from gas to water. Further experiments could be made to investigate how the water droplet size and growing surface area affect the efficiency of PCD process.

Experiments with PCD reactor were made with four pulse frequencies. It was discovered that with higher pulse frequencies result in more efficient removal of toluene. The highest toluene removal efficiency of 63 % was achieved with 800 pps corresponding to the output power of 100 W. The overall toluene removal efficiency reached up to 12.70 $g \cdot kWh^{-1}$ using 200 pps which corresponds to output power of 25 W. The lowest energy efficiency (6.44 $g \cdot kWh^{-1}$) was achieved with 800 pps. Thus, an optimal pulse frequency and energy input should be determined based on required removal efficiency and energy consumption.

Another aspect to be considered is the generation of ozone in PCD process. Higher pulse frequency contributes to ozone production in large quantities. On one hand ozone is considered as air pollutant and its generation in PCD causes secondary pollution. On the other hand ozone was found to enhance toluene degradation by applying PCO as a post treatment method. An average toluene removal efficiency by PCO was found to be 27.2 %.

Ozone conversion with PCO was studied and a linear dependency between residence time and concentration was found. This linear trend was explained in terms of mass balance in an ideal plug flow reactor using Langmuir-Hinshelwood kinetic model of heterogeneous catalysis. As a result, a pseudo-zero order reaction for ozone conversion was observed in the PCO reactor. Ozone removal efficiency of 23 % was achieved with the photocatalytic reactor.

Finally, price for toluene removal and ozone conversion was calculated based on the energy consumption of both PCD and PCO processes. The cheapest PCD process was found to cost 0.009 € and 0.16 € per gram of toluene and ozone removed, respectively. Toluene removal was approximately 20 times cheaper than the ozone conversion.

Further research should be focused on the optimization of process parameters and design of the PCD reactor. An optimized ratio between pollutant removal in PCD reactor and the energy input should be identified. Optimal ozone concentration should be established keeping in mind on one hand the importance of ozone during PCO and on the other the energy demand for ozone conversion back to oxygen. Furthermore, the removal of mixture of pollutants is of a high interest for further investigation.

SUMMARY

The main objective of the present thesis was to investigate the toluene degradation in pulsed corona discharge (PCD) reactor followed by photocatalytic oxidation (PCO). Literature review consists of the description of the characteristics of toluene, its sources, concentrations in urban and domestic air, health impact and related regulations. Furthermore, currently available technologies for VOC removal such as incineration, thermal catalytic oxidation, absorption, adsorption, condensation, and biological treatment are discussed. In experimental part air was artificially polluted with toluene with subsequent PCD treatment. During PCD treatment ozone is generated and being an air pollutant requires corresponding removal. Conversion of ozone to oxygen in PCO reactor was examined.

The most important results of the study include the mass-transfer of toluene from air to circulation waster. Mass-transfer coefficient was derived from a linearization of a toluene saturation curve. In the PCD reactor, the highest toluene removal efficiency of 63 % was achieved with 800 pulse per seconds (pps). With respect to PCO treatment, an average toluene removal was found to be 27 %. The overall energy efficiency of toluene removal reached up to 12.70 $g \cdot kWh^{-1}$ with 200 pps.

Ozone conversion with PCO was studied and a linear trend as a function of residence time in the PCO reactor was observed and explained in terms of mass balance in an ideal plug flow reactor. Ozone conversion efficiency of 23 % was achieved with the photocatalytic reactor.

Finally, a price for toluene removal and ozone conversion was determined based on the energy demand of PCD and PCO processes considering current price for electricity. The cheapest prices for toluene and ozone removal were found to be 0.009 € and 0.16 € per gram, respectively. Toluene removal was approximately 20 times cheaper than that of the ozone conversion.

For further research, additional focus should be given to the optimization of the process parameters and design of the PCD reactor. The combination of PCD and PCO has shown its great potential and thus requires upscaling studies using real sources of pollution.

KOKKUVÕTTE

Käesoleva lõputöö peamine eesmärk oli uurida tolueeni lagundamist koroona-impulss elektrilahendusega (KIEL), millele järgneb fotokatalüütiline oksüdatsioon (FKO). Kirjanduse ülevaade koosnes tolueeni omaduste, selle tekkeallikate, kontsentratsioonide sise- ja välisõhus, tervisemõju ja sellega seotud õigusaktide kirjeldusest. Lisaks käsitleti olemasolevaid tehnoloogiaid lenduvate organiiliste ühendite (LOÜ) eemaldamiseks õhust. Nende hulgas on termiline ja katalüütiline põletamine, absorptsioon, adsorptsioon, kondenseerimine ja bioloogiline töötlemine.

Katse käigus reostati õhku kunstlikult tolueeniga, millele järgnes KIEL töötlus. Siin tuleks mainida et KIEL töötluse käigus tekib osoon, mis on teadaolevalt õhusaasteaine ja seega vajab samuti eemaldamist õhust. Osooni lagundamiseks kasutati fotokatalüütilist protsessi.

Uuringu kõige olulisemad tulemused hõlmavad tolueeni massiülekande protsessi õhust KIEL retsirkulatsioonivette. Massiülekande koefitsient tuletati tolueeni küllastumiskõvera lineariseerimise teel. Kõrgeim tolueeni eemaldamaise effektiivsus KIEL reaktoris oli 63 %, kasutades 800 impulssi sekundis (pps). FKOga õhutöötlemisel leiti, et keskmine tolueeni eemaldamine oli 27 %. Tolueeni eemaldamise üldine energiatõhusus ulatus 200 pps puhul 12,70 $g{\cdot}kWh^{-1}$-ni.

Lisaks tolueeni oksüdeerimisele uuriti osooni lagundamist FKOga ning avastati lineaarset sõltuvust viibimise aja ja osooni konsetratsiooni vahel. Käesolevat fenomeeni seletati pideva reaktori massibilansi abil. Fotokatalüütilise reaktori kasutamisel saavutati osooni lagundamise effektiivsus väärtusega 23 %.

Lõpuks määrati tolueeni ja osooni eemaldamise hind, mis põhineb KIEL ja FKO protsesside energiatarbel, ja võttes arvesse kehtiva elektrihinda. Tolueeni ja osooni eemaldamise odavaimad hinnad olid vastavalt 0,009 eurot ja 0,16 eurot grammi kohta. Tolueeni eemaldamine oli ligikaudu 20 korda odavam kui osooni lagundamine.

Tulevikuuuringutes tuleks täiendavalt keskenduda protsessi parameetrite optimeerimisele. KIEL ja FKO kombinatsioon on näidanud suurt potentsiaali ja seega on vaja laiendada uuringuid, kasutades reaalseid saasteallikaid.

LIST OF REFERENCES

Agency for Toxic Substances and Disease Registry (ATSDR) (2017) Toxicological profile for Toluene. Atlanta, GA: U.S. Department of Health and Human Services, Public Health Service.

Ajo, P., Kornev, I., & Preis, S. (2017) Pulsed Corona Discharge Induced Hydroxyl Radical Transfer Through the Gas-Liquid Interface. Scientific Reports, 7(1). https://doi.org/10.1038/s41598-017-16333-1

Altof, K., Krichevskaya, M., Preis, S., Tähemaa, T., Bolobajev, J. (2023) Ozone-assisted degradation of 2-methoxyethanol in a prototype plug flow photocatalytic reactor, Chemical Engineering Journal, doi: https://doi.org/10.1016/j.cej.2023.148488

Biard, P.-F., Bouzaza, A., & Wolbert, D. (2007) Photocatalytic Degradation of Two Volatile Fatty Acids in an Annular Plug-Flow Reactor; Kinetic Modeling and Contribution of Mass Transfer Rate. Environmental Science & Technology, 41(8), 2908–2914. https://doi.org/10.1021/es062368n

Bolden, A.L., Kwiatkowski, C.F., and Colborn, T. (2015) 'New Look at BTEX: Are Ambient Levels a Problem?', *Environmental Science & Technology*, 49(9), pp. 5261–5276. Available at: https://doi.org/10.1021/es505316f.

Boyjoo, Y. et al. (2017) A review on photocatalysis for air treatment: From catalyst development to reactor design. Chemical engineering journal (Lausanne, Switzerland: 1996). [Online] 310537–559.

Cheng, M. and Brown, S.K. (2003) VOCs identified in Australian indoor air and product emission environments. In Proceedings of National Clean Air Conference (Vol. 2003, pp. 23-27).

Chiang, P.-C. & Gao, X. (2022) Air Pollution Control and Design. 1st edition. [Online]. Singapore: Springer.

European Environment Agency (EEA) (2023) *Air pollution in Europe: 2023 reporting status under the National Emission reduction Commitments Directive*.

Feng, X. *et al.* (2018) ‘Synergistic effects and mechanism of a non-thermal plasma catalysis system in volatile organic compound removal: a review’, *Catalysis Science & Technology*, 8(4), pp. 936–954. Available at: https://doi.org/10.1039/C7CY01934C.

Frascari, D. et al. (2019) Continuous flow adsorption of phenolic compounds from olive mill wastewater with resin XAD16N: life cycle assessment, cost–benefit analysis and process optimization. Journal of Chemical Technology & Biotechnology. [Online] 94 (6), 1968–1981.

Geiss, O. et al. (2011) The AIRMEX study - VOC measurements in public buildings and schools/kindergartens in eleven European cities: Statistical analysis of the data. Atmospheric environment (1994). [Online] 45 (22), 3676–3684.

Gong, J.-Y., Chen, Y.-C. and Yu, K.-P. (2017) “Photocatalytic decomposition of indoor ozone motivated by the white-light-emitting diode,” *Clean technologies and environmental policy*, 19(10), pp. 2393–2404.

Gottschalk, C. et al. (2000) Ozonation of Water and Waste Water: A Practical Guide to Understanding Ozone and Its Application. 1st edition. [Online]. Hoboken: John Wiley & Sons, Incorporated.

He, C. *et al.* (2019) Recent Advances in the Catalytic Oxidation of Volatile Organic Compounds: A Review Based on Pollutant Sorts and Sources’, *Chemical Reviews*, 119(7), pp. 4471–4568. Available at: https://doi.org/10.1021/acs.chemrev.8b00408.

Hernández-Alonso, M. D. et al. (2011) Operando FTIR study of the photocatalytic oxidation of methylcyclohexane and toluene in air over TiO2–ZrO2 thin films: Influence of the aromaticity of the target molecule on deactivation. Applied catalysis. B, Environmental. [Online] 101 (3–4), 283–293.

Kanazawa, S., Kawano, H., Watanabe, S., Furuki, T., Akamine, S., Ichiki, R., Ohkubo, T., Kocik, M., & Mizeraczyk, J. (2011) Observation of OH radicals produced by pulsed discharges on the surface of a liquid. Plasma Sources Science and Technology, 20(3), 034010. https://doi.org/10.1088/0963-0252/20/3/034010

Mo, J. et al. (2009) Photocatalytic purification of volatile organic compounds in indoor air: A literature review. Atmospheric environment (1994). [Online] 43 (14), 2229–2246.

Mudliar, S. et al. (2010) Bioreactors for treatment of VOCs and odours – A review. Journal of environmental management. [Online] 91 (5), 1039–1054.

National Institute for Occupational Safety and Health (NIOSH) (1994) Immediately dangerous to life or health concentrations (IDLH): Toluene. [Online] Available at: https://www.cdc.gov/niosh/idlh/108883.html

National Institute of Standards and Technology (NIST) (2023) Toluene: Henry's Law data. [Online] Available at: https://webbook.nist.gov/cgi/cbook.cgi?ID=C108883&Units=SI&Mask=10#Solubility

Noll, K. (1999) Fundamentals of air quality systems: Design of air pollution control devices. Annapolis (Md.): American Academy of Environmental Engineers.

Ollis, D.F., 2005. Kinetic disguises in heterogeneous photocatalysis. Topics in catalysis, 35(3-4), pp.217-223.

Ono, R., & Oda, T. (2003) Dynamics of ozone and OH radicals generated by pulsed corona discharge in humid-air flow reactor measured by laser spectroscopy. Journal of Applied Physics, 93(10), 5876–5882. https://doi.org/10.1063/1.1567796

Panorel, I. Cherry. (2013) Pulsed corona discharge as an advanced oxidation process for the degradation of organic compounds in water. Lappeenranta: Lappeenranta University of Technology.

Sharma, Nikhil. et al. (2018) Air Pollution and Control. Singapore: Springer Singapore, 2018. Web.

United States Environmental Protection Agency (2023) Health Effects of Ozone Pollution. [Online] Available at: https://www.epa.gov/ground-level-ozone-pollution/health-effects-ozone-pollution

Wallenius K, Hovi H, Remes J, Mahiout S, Liukkonen T. (2022) Volatile Organic Compounds in Finnish Office Environments in 2010–2019 and Their Relevance to Adverse Health Effects. International Journal of Environmental Research and Public Health. [Online] 19 (7), 4411. https://doi.org/10.3390/ijerph19074411

Wang, S. et al. (2007) Volatile organic compounds in indoor environment and photocatalytic oxidation: State of the art. Environment international. [Online] 33 (5), 694–705.

Xu, H. et al. (2023) A complementary VOCs recovery system based on cryogenic condensation and low-temperature adsorption. International journal of refrigeration. [Online] 153222–230.

Zhang, Z. et al. (2023) Insights into the reaction mechanism of toluene oxidation by isotope dynamic experiment and the kinetics over MCeZr/TiO2 (M = Cu, Mn, Ni, Co and Fe) catalysts. Fuel (Guildford). [Online] 341127760-.

Zhou, W. et al. (2023) Catalytic Oxidation Mechanism of Toluene over Ce x Mn 1- x O 2: The Role of Oxygen Vacancies in Adsorption and Activation of Toluene. Langmuir. [Online] 39 (24), 8503–8515.